Global Ecology and Biogeography

Old growth Afrotropical forests critical for maintaining forest carbon

Journal:	*Global Ecology and Biogeography*
Manuscript ID	GEB-2020-0089.R1
Manuscript Type:	Research Papers
Keywords:	tropical forest, Gabon, Central Africa, aboveground biomass, carbon, large trees, tree height, wood density, climate change

SCHOLARONE™
Manuscripts

ABSTRACT

Aim: Large trees (≥70 cm DBH) contribute disproportionately to aboveground carbon stocks (AGC) across the tropics but may be vulnerable to changing climate and human activities. Here we determine the distribution, drivers, and threats to large trees and high-carbon forest in Central Africa.

Location: Central Africa

Time Period: Current

Major taxa studied: Trees

Methods: Using Gabon's new National Resource Inventory of 104 field sites, AGC was calculated from 67,466 trees from 578 species and 97 genera. Power and Michaelis-Menten models assessed the contribution of large trees to AGC. Environmental and anthropogenic drivers of AGC, large trees, and stand variables were modeled using AIC weights to calculate average regression coefficients for all possible models.

Results: Mean AGC for trees ≥10 cm diameter-at-breast height in Gabonese forestlands was 141.7 [95% CI: 1301, 153.3] Mg C ha^{-1}, with an average of 166.6 [150.2, 183.1] Mg C ha^{-1} in old growth forest, 171.3 [154.8, 187.7] Mg C ha^{-1} in concession forest, and 96.6 [77.0, 116.2] Mg C ha^{-1} in secondary forest. High carbon forests occurred where large trees are most abundant: 31% of AGC was stored in large trees (2.3% of all stems). Human activities largely drove variation in AGC and large trees, but climate and edaphic conditions also determined stand variables (basal area, tree height, wood density, stem density). AGC and large trees increased with distance from human settlements; AGC was 40% lower in secondary than primary and concession forests and 33% higher in protected than non-managed areas.

Main conclusions: AGC and large trees were negatively associated with human activities, highlighting the importance of forest management. Redefining large trees as ≥50 cm DBH (4.3% more stems) would account for 20% more AGC. Efforts to reduce tropical carbon emissions have largely focused on deforestation and reforestation. This study demonstrates that protecting relatively undisturbed forests can be disproportionately effective in conserving carbon and suggests that including sustainable forestry in programs like REDD+ could maintain carbon dense forests in logging concessions that are a large proportion of remaining Central African forests.

For Peer Review

INTRODUCTION

Large trees dominate intact tropical ecosystems, bolstering global biodiversity and carbon storage (Lewis *et al.* 2015; Sullivan *et al.* 2017). Rising above the canopy, they modulate the understory microclimate and provide habitat and resources for animals, invertebrates, and plants like epiphytes and lianas (Poulsen *et al.* 2017), while storing a large fraction of forest carbon (Stegen *et al.* 2011; ter Steege *et al.* 2013; Bastin *et al.* 2015). The world's tallest and densest forests are temperate rainforests, but tropical forests are the most widespread, accounting for two-thirds of all terrestrial biomass (Pan *et al.* 2013). Large trees, often defined as ≥70 cm diameter-at-breast height (DBH), comprise on average 25-45% of AGC in tropical regions while representing a small fraction of stems (Slik *et al.* 2013). Paleotropical forests typically have larger trees than Neotropical forests, with African trees tending to have larger diameters and Asian trees tending to be taller than South American trees (Banin *et al.* 2012); but hotspots of biomass occur regionally, including the Guyana shield, intact forests of Borneo and Papua New Guinea, and central and western parts of the Congo Basin (Lewis *et al.* 2013; Slik *et al.* 2013; Xu *et al.* 2017). Given the importance of large trees for forest structure and functioning, and their sensitivity to disturbance, a primary goal of forest ecology is to identify the distribution, drivers, and threats to the world's large forests (Lindenmayer *et al.* 2012).

The influence of large trees on forest structure suggests that variables that affect the abundance of large stems could strongly influence ecosystem function and carbon storage. Multiple studies demonstrate that environmental variables, such as climate and soils, drive variation in tropical AGC, and to a lesser extent numbers of large trees, but their importance varies across regions and contexts. Forests in Africa, but not other regions, show a negative correlation between temperature and AGC (Lewis *et al.* 2013; Slik *et al.* 2013; Xu *et al.* 2017). The importance of annual precipitation and rainfall seasonality for AGC has been highlighted by several studies (Malhi *et al.* 2006; Slik *et al.* 2010; Chave *et al.* 2014a), including for African forests that often have lower average rainfall than other regions (Lewis *et al.* 2013; Slik *et al.* 2013), although precipitation in the wettest three months may be negatively associated with AGC above a certain point (Lewis *et al.* 2013; Xu *et al.* 2017). The positive effect of annual precipitation is consistent with reports that large trees are sensitive to water stress (Slik 2004; Van Nieuwstadt & Sheil 2005) due to a loss of hydraulic conductivity as the water deficit increases (Stegen *et al.* 2011). Using tree height as an indicator of large trees and AGC, a comparison of all humid tropical forests found that dry season precipitation and maximum annual water deficit are important determinants of height, but surface topography and topsoil texture also correlate strongly with the distribution of large trees (Yang *et al.* 2016). Generally, AGC increases with soil fertility in tropical forests (Quesada *et al.*

For Peer Review

2012), although studies have found weak effects of soils, which have been partially attributed to the poor data quality of global soil databases (Lewis *et al.* 2013a; Slik *et al.* 2013a).

Rarely tested at large scales (regionally or nationally) in the humid tropics (Berenguer *et al.* 2014), human activities can have strong effects on large trees and AGC. Deforestation, usually caused by the conversion of forest to cropland and pasture, reduces the extent and biomass of the entire forest (Gibbs *et al.* 2010). Other forms of natural and anthropogenic disturbance disproportionately affect large trees. Logging is widespread across the tropics, occupying 26% of Central Africa's remaining forests and up to 74% of some countries (Bayol *et al.* 2012). Timber operations harvest the largest most valuable trees, including many Central African biomass hyperdominants (Bastin et al. 2015). Land clearing for settlement and subsistence agriculture follows on the heels of logging, resulting in the intentional removal of large trees (Lindenmayer *et al.* 2012). While logging and subsistence agriculture clearly reduce carbon stocks (Medjibe *et al.* 2013), their effects on large trees and AGC remain mostly unstudied at the landscape scale.

Here we report on one of the first modern forest inventories of a tropical forested country -- the Gabonese Republic in Central Africa (Figure 1). Gabon is the second most forested country in the world, with 87% forest cover, a deforestation rate near zero, and 67% of its forests in timber concessions (Forêt Ressources Management 2018). For economic development the government seeks increased investment in industrial agriculture and logging, while committing to reduce greenhouse gas emissions and preserve ecosystems and biodiversity. We use Gabon's national resource inventory (NRI) to characterize forest structure, quantify carbon stocks and identify areas of high carbon as priorities for conservation. We investigate: (1) the carbon density of forests across Gabon; (2) the contribution of large trees to AGC; and (3) the relative effects of environmental and anthropogenic variables on forest structure, with a focus on AGC and large trees.

For Peer Review

MATERIALS AND METHODS

Located on the western coast of equatorial Africa, Gabon is part of the Congo Basin forest, although its waters drain into the Ogooué Basin (Figure 1a). A strong precipitation gradient extends from the northern coast (3200 mm annually) to the interior (1300 mm) of the country. Land cover is dominated by rain forest (76%), followed by cropland (10%), grassland and savanna (7%), and flooded broadleaf forest (5%) (World Resources Institute 2017). Four ecosystem types dominate (Figure 1d). *Coastal evergreen rainforest* in the west (0-300 m elevation) includes a mixture of *terra firma*, mangroves, flooded forest, and *Raphia* swamps. Coastal forests have been heavily harvested and reduced to secondary forest, with exceptions such as the Mondah and Mayumba forests and the Gamba Complex.

Coastal forest transitions into low elevation *central forest*, where the sedimentary basin meets older geological types giving way to the Chaillu mountain chain – a block of sedimentary rock with a maximum elevation of 1020 m. Central forest (300-1000 m), often dominated by the long-lived pioneer timber species, *Aucoumea klaineana* (okoumé), covers most of central Gabon and is indicative of disturbance in the last 150 years (Born et al. 2011). The *northeastern lowland forest* (300-1000 m) extends east of the *Aucoumea* distribution. This semi-deciduous forest is characterized by a predominance of tree species such as *Terminalia superba* (limba), *Millettia laurentii* (wenge), and *Celtis* spp. The rest of the county is covered by *savanna* that is often interrupted by forest-savanna mosaic, with continuous savanna in the southwest and southeast.

Gabon's timber concessions include14.7 million ha of forest, with 74% of the area under management plans and 16% certified for sustainable management (Forêt Ressources Management 2018). Average harvest intensity is low, but varies with logging technique and history (Medjibe *et al.* 2013). By contrast, commercial agriculture is currently very limited in scope (Austin *et al.* 2017; Tyukavina *et al.* 2018). Secondary forests recovering from slash-and-burn agriculture or other forms of deforestation are located near towns and villages and along roads, particularly the paved national roads connecting regional capitals. Several types of formal land management exist in Gabon: `protected` refers to areas under strictest management, including national parks, presidential reserves and arboretums (15 parks, 3.3. million ha); 'reserve' designates Ramsar sites with lower levels of protection than national parks (6 sites, 2,215,954 ha); 'buffer' signifies 5-km buffer zones around national parks'; 'hunting' signifies designated hunting reserves (5 hunting reserves, 497,500 ha); and, 'none' indicates no formal management.

Inventory Design, Data Collection, and Estimation of AGC

Gabon's NRI is based on a semi-systematic sample of forestlands. We divided the country into 135 - 50 x 50 km cells and randomly located an inventory site within each cell using the Reverse Randomized Quadrant-Recursive Raster (RRQRR) algorithm in GIS (Figure 1c). The algorithm uses a spatially balanced design for sampling that maximizes the spatial independence among sample locations (Theobald *et al.* 2007). Stratified sampling is often more efficient than random sampling, but we lacked rigorous, *a priori* data for the selection of strata. Our semi-systematic approach does not depend on external data and samples can be added without disturbing the statistical integrity of the design.

Each inventory site consisted of one 1-ha (100 x 100 m) plot and four 0.16-ha (40 x 40 m) satellite plots spaced 250 m apart, with two satellite plots located to the east and west of the permanent plot. We employed this winged design to evaluate local variation in forest structure. Of 135 original

For Peer Review

sampling sites, we discarded 16 located in the ocean and did not sample 15 in savanna unlikely to have trees ≥10 cm DBH. At 16 sites, fewer than four satellite plots were established because they were in water bodies, open grassland, or the work was cut short for logistical reasons (e.g. sick field technician). Between 2012-2014 four field teams of five trained technicians inventoried the trees using standard protocols for plot establishment and measurement. Each tree ≥10 cm DBH was mapped, measured and identified. Measured trees in permanent plots, but not satellite plots, were marked with aluminum tags. Field teams measured tree diameters, *D*, at a height of 1.3 m from the ground or 50 cm above any buttresses, stilt roots, or deformities. They measured tree heights with a laser hypsometer (TruPulse 200 Hypsometer, Laser Technology, Inc., Centennial, CO, USA), taking three measurements of 55 randomly selected trees per site with 10 trees from each of 5 DBH subclasses (10-20 cm, 21-30 cm, 31-40 cm, 41-50 cm, >50 cm) and the five largest trees (e.g., Sullivan *et al.* 2018). Samples of unidentified trees were taken to the National Herbarium for identification. Of 67,466 trees, 80.9% were identified to species and 99.4% to genus; of 1572 large trees, 92.1% were identified to species and 99.6% to genus.

We estimate AGC from tree measurements in 104 forest sites by converting tree diameters, D, to aboveground biomass (AGB) using allometric equations for moist forests (1500-3500 mm precipitation yr^{-1}) that incorporate terms for wood density, ρ, and tree height, H (Appendix S1 in Supporting Information). In the case of multi-stemmed trees, we applied the model to each stem. These equations include the pantropical model (Chave *et al.* 2014b),

$$\mathrm{AGB_{est}} = 0.0673 \times (\rho \mathrm{D}^2 \mathrm{H})^{0.976} \tag{1}$$

and a Gabon-specific model (Ngomanda *et al.* 2014),

$$\mathrm{AGB_{est}} = \exp(-2.5680 + 0.9517(\ln(\mathrm{D}^2 \times \mathrm{H})) + 1.1891(\ln \rho)). \tag{2}$$

Other allometric equations exist, but we focus on the pantropic model to facilitate comparison with other studies and because it is derived from many trees and species including 1429 harvested trees from Africa. The Gabon-specific allometric model is based on 10 species (101 trees) from a single site in northeastern Gabon (Ngomanda *et al.* 2014). Our study includes many families and species from across Gabon, making the pantropic equation more appropriate.

We used the best taxonomic match of wood density for each stem (Zanne *et al.* 2009), substituting the mean wood density of the plot in the absence of species, genus, or family-level information. Of all inventoried trees, 41.9% had wood density values at the species level, and 24.1%, 12.2%, and 21.9% matched at the genus, family, and plot levels. Of large trees, 63.7% had wood density values at the species level, and 20.8, 4.5, and 11.0% matched at the genus, family, and plot levels. With height measurements for 7,036 trees, we built a series of diameter-height (D:H) regression models

For Peer Review

(linear, quadratic and polynomial) for each plot to predict the heights of the unmeasured trees (Beirne *et al.* 2019). For two plots without height measurements, we applied a national D:H model fitted to all the NRI data:

$$\widehat{H} = 43.98 - 35.38 \times e^{-0.019D} \tag{3}$$

AGC was calculated by summing the AGB of all the stems in a plot, dividing by plot area and multiplying by the assumed carbon content, 47.1%, of AGB (Thomas & Martin 2012). Throughout, we present the area-weighted carbon density for each site (1-ha plot and satellite plots) as Mg C ha^{-1}.

Importance of Large Trees to AGC

To assess the contribution of large trees to AGC, we applied Bastin et al.'s (2015) model to estimate plot-level AGB, $\widehat{\mathrm{AGB}}_{\mathrm{TOT}}$, from the AGB of the largest trees, X:

$$\widehat{AGB}_{TOT} = \alpha_i \times X^{\beta_i}. \tag{4}$$

The power model coefficient, α, is predicted from the number, i, of the largest trees using a power regression model with no intercept:

$$\alpha_i = a_1 x_i^{b_1}. \tag{5}$$

The exponent, β, is predicted from the number, i, of the largest trees using a Weibull model:

$$\beta_i = a_2 - b_2 e^{\left(c_2 * x_i^{d_2}\right)}. \tag{6}$$

We fit the models to the entire dataset and each disturbance type separately as forests might accumulate AGC from large trees at different rates (Appendix S2). To test whether the contribution of large trees differs among disturbance types, we modeled the relationship between the proportion of explained variation and cumulative number of trees with the Michaelis-Menten function:

$$\hat{R}^2 = \frac{f + (x_i + j)}{g(x_i + j)} \tag{7}$$

where f, g, and j are fitted parameters. We chose the asymptotic Michaelis-Menten (MONOD) growth function for its simplicity and use in assessments of biomass growth (McMahon *et al.* 2010; Zhu *et al.* 2018). We fitted a single general model to the entire dataset, and then compared its fits to data subsetted by disturbance type with individual models for each disturbance type using AICc.

Drivers of AGC, Large Trees, and Stand Variables

We downloaded bioclimatic variables from the WORLDCLIM dataset (http://www.worldclim.org/; Hijmans *et al.* 2005), defining the center of a plot as its location, and compiling the following: average annual temperature (° C), temperature of the warmest quarter (° C), temperature of the coldest quarter (° C), temperature seasonality (standard deviation of temperature), annual rainfall (mm), rainfall in wettest

For Peer Review

quarter (mm), rainfall in the driest quarter (mm), and rainfall seasonality (CV of rainfall). Several climate variables were strongly correlated ($r \geq 0.70$), therefore we used principal components analysis (PCA) to reduce them to three linearly uncorrelated variables that explained 95.0% of the variance in climate data (Appendix S3). Climate axis 1 (53.4% variance), *Pdryq*, was positively correlated with driest quarter and negatively related to all other variables. Axis 2 (22.2% variance), *Pseas*, was positively related to seasonality in temperature and precipitation and negatively related to all other variables. Axis 3 (19.3% variance), *Precip*, was strongly positively correlated with total precipitation and rainfall in wettest quarter.

Similarly, we selected 15 soil variables from the UN Food and Agriculture Organization (FAO) database (see (FAO 2002) for exact definitions of variables). Using PCA, we summarized the soil data in three independent axes that explained 83.6% of the variance in soil data (Appendix S3). Soil axis 1 (47.1% variance), soil fertility, *Sfert*, was positively correlated with organic carbon topsoil, organic carbon subsoil, soil production, cation exchange capacity (CEC) soil and CEC clay. Axis 2 (21.7% variance), soil depth, *Sdepth*, was negatively correlated with nitrogen topsoil and C:N ratio topsoil, but positively correlated with soil depth, available water, and pH topsoil. Axis 3 (14.8% variance), *Sdrain*, which we interpret as soil drainage and oxygen availability to roots, was positively correlated with soil drainage and textural classes of topsoil and subsoil, but negatively correlated to C:N ratio, base saturation topsoil, and CEC clay topsoil.

For Peer Review

We evaluated several indictors of disturbance, including disturbance type (concession, primary, secondary; Figure 1e), distance from nearest village (km), and presence of human trails. Primary, or old growth, forest was defined as having no recent obvious signs of disturbance. Concession forest included sites with obvious logging damage and within timber concessions. Secondary forest was defined as recovering from slash-and-burn agriculture or other forms of deforestation. Technicians recorded disturbance type and presence of human trails in the field, whereas the Euclidean distance from the plot center to the nearest village was calculated in R. Finally, we classified plots into four major ecosystems (coastal forest, central forest, and northeastern forest, and savanna; Figure 1) and four habitats (highland, swamp, flooded, and *terra firma*).

We explored the data by examining bivariate relationships between independent variables and response variables (AGC, number of large trees, and stand variables; Figure 2). We used linear regression for all normally distributed response variables and generalized linear models for counts of large trees, accounting for overdispersion with a quasipoisson model. We then examined multivariate relationships among the above explanatory variables, standardized to facilitate comparison of effect sizes, and response variables using model averaging, implemented through the MuMIn package (Barton

2019). Model averaging executes models for all possible combinations of variables (i.e. 4,095 combinations for our 12 variables) and ranks them from best to worst according to their AICc scores. We considered all models with Δ AICc < 4 as equally informative and determined the support for the explanatory variables by calculating their frequency of occurrence in the models (Galipaud *et al.* 2017). We used a cut-off of 60% support in our discussion of variables that drive numbers of large trees and AGC. Model-averaged regression coefficients based on AICc weights have been shown to be incorrect estimates of partial effects for individual predictors when there is multicollinearity among predictor variables (Cade 2015); but, as described above, we minimized multicollinearity by using PCA to reduce multiple correlated variables to fewer non-correlated predictors. All statistical analyses were conducted in R version 3.5.0 (R Core Team 2018).

RESULTS

National Assessment of AGC

NRI sites represented the forest types in Gabon (Table 1, Figure 3) and differed in AGC and stand variables (Appendix S1). Mean AGC across all 104 forestland sites was 141.7 ± 60.4 (SD) Mg C ha^{-1} (range: 3.6 to 292.5) (Table 1): the lowest AGC occurred in a coastal swamp, whereas 7 of the 9 lowest AGC sites occurred in savanna forest. Estimates of AGC from satellite plots were marginally less than adjacent 1-ha plots (lmm: $\beta = 23.9$, $t = 1.77$, $p = 0.078$). The average distance between NRI sites was 31.9 km ± 12.6 and site-level AGC was not spatially autocorrelated (Morans $I = -0.005$, $p = 0.787$). When treated as independent replicates, satellite and permanent plots were significantly spatially autocorrelated (Morans $I = 0.306$, SD = 0.027, $p < 0.001$), indicating that AGC is less variable within sites than among sites and that site is the appropriate level of replication. Primary and concession forest contained significantly more AGC than secondary forest (Table 1). AGC was highest in the northeast forest ecosystem and lowest in savanna forest and significantly higher on highlands than swamps and flooded forests. Protected areas held 46.3% more AGC than non-managed areas, but not significantly more than buffer zones, hunting zones, or reserves (Figure 3).

The best single predictor of site-level AGC was the AGC of large trees ($R^2 = 0.728$), followed by basal area ($R^2 = 0.692$), number of large trees ($R^2 = 0.561$) and tree height ($R^2 = 0.525$; Figure 2; Appendix S1). When combined, basal area, tree height, basal area-weighted wood density, and number of trees contributed significantly to site-level AGC ($F_{4,99} = 345.8$, $R^2 = 0.931$, $p < 0.001$; see results of large trees below), accounting for 93.6% of variation in AGC. Basal area, $\overline{BA}$, had the strongest positive effect on AGC, followed by mean tree height, $\overline{H}$, and wood density, $\bar{\rho}$; whereas, the number of trees at a

For Peer Review

site, T, negatively affected AGC: ($y = 66.7 + 18.9X_{\overline{BA}} + 11.5_{\overline{H}} + 5.6_{\overline{\rho}} - 3.9_{T}$). High AGC occurred along the southwest coast of Gabon, stretching along the sedimentary basin from Port Gentil to Mayumba ($\overline{AGC}$ = 209.1 Mg C ha^{-1}, N = 8; Figure 4) and in the northeast in and around the Ivindo and Mwagna National Parks ($\overline{AGC}$ = 193.8 Mg C ha^{-1}, N = 11; Figure 4). Highest numbers of large trees occurred in the north and northeast ($\overline{N}_{trees} = 22$, N = 11; Figure 4), whereas plots near the coast contained few large trees ($\overline{N}_{trees} = 11.6$, N = 9).

Importance of Large Trees to AGC

Most AGC in Gabon's forests was stored in a limited number of large trees. Small trees (<40cm DBH) accounted for 88.5% of all trees, but only 36.3% of AGC; whereas large trees (≥70 cm DBH) made up 2.3% of trees and 30.6% of AGC, and the largest trees (>100 cm DBH) represented 0.48% of trees and 12.1% of the AGC (Appendix S2). The proportion of AGC per site increased rapidly with the cumulative addition of the largest trees, reaching an average of 50% ± 27% for the 30 largest trees (~5% of stems) and 78% ± 36% for the 100 largest trees (~24% of the stems; Figure 5). The largest 10 and 20 trees explained 81% and 87% of the variance in AGC ($rRSE_{top10}$ = 20%; $rRSE_{top20}$ = 16%), and 69 trees, 16.6% of stems, explained 95% of the variation on average (Appendix S2). The largest 20 trees in a plot explained different levels of variation in AGC depending on disturbance type (concession = 84%, primary = 81%, and secondary = 91%). Our Michaelis-Menten models similarly demonstrated that secondary forest accumulates AGC faster from large trees than primary and concession forest (Appendix S2).

Thirty-five tree species (6.1% of identified species) made up 50% of total AGC. Species of large trees varied by ecosystem: *Aucoumea klaineana* (13-23% of large trees) is the most abundant species in coastal, central, and savanna forests, whereas *Gilbertiodendron dewevrei*, *Scyphocephalium* spp., *Petersianthus macrocarpus* and *Maranthes glabra* make up 18.6% of Congolian forest (Appendix S2). The composition of large tree species was generally the same across disturbance types, except secondary forest had significantly higher average numbers of *Musanga cecropioides* (16.5 stems vs. 3.5 in concession and 1.1 in primary forest) and *Aucoumea klaineana* (19.2 stems vs. ~5.8 in concession and primary forest). Biomass hyperdominants included *Aucoumea klaineana*, *Scyphocephalium mannii*, *Desbordia glaucescens*, *Pycnanthus angolensis*, and *Piptadeniastrum africanum*. *Aucoumea klaineana*, which comprises 80% of Gabon's timber exports (Lescuyer *et al.* 2011), represented 4.7% of total AGC and 9.1% of the AGC of large trees. Several of the ten most abundant large tree species are harvested for timber (Appendix S2).

For Peer Review

Drivers of Large Trees and AGC

Using model averaging to evaluate the leading climatic, environmental, and human determinants of forest structure (AGC, number of large trees, and stand variables; Figure 6; Appendix S3), the independent variables most frequently retained in the top models included: distance from village, disturbance type, (5 response variables), ecosystem type (4 response variables), slope and precipitation (3 response variables). Human activity negatively affected stand variables. Apart from stem density, all stand variables had lower values in secondary than primary and concession forest and increased with distance from village. Annual precipitation positively affected most stand variables, but wood density decreased with precipitation. Mean wood density and basal area increased with slope, whereas tree height decreased with slope. Here we focus on AGC and large trees (see Supplementary 3 for other response variables).

Variation in site-level AGC across Gabon was explained by 29 equally likely models (mean R^2 = 0.346) and was most frequently positively correlated with distance from village and soil fertility (Figure 6, Table 3, Appendix S3). Secondary and savanna forests had significantly lower AGC than other disturbance and ecosystem types

Variation in site-level number of large trees was explained by 51 equally likely models (mean R^2 = 0.508). The number of large trees was positively related to distance from village (Figure 6). The number of large trees was significantly lower in secondary forest (7.8 large trees ha^{-1}) than concession (12.4 trees ha^{-1}) and primary forest (10.5 trees ha^{-1}).

DISCUSSION

National Assessment of AGC

Gabon has one of the highest densities of aboveground forest carbon among forested nations (Saatchi *et al.* 2011), with a national average of 141.7 Mg C ha^{-1} [95% CI: 130.1, 153.3]. By comparison, mean AGC of the Democratic Republic of Congo (DRC), also from a systematic sampling of forests, is 113 ± 9 Mg C ha^{-1} (Xu *et al.* 2017). On average, the primary forests of Gabon have a carbon density (~150 Mg C ha^{-1}) similar to the DRC and much higher than old growth forests in Amazonia and southeast Asia (Feldpausch *et al.* 2012; Lewis *et al.* 2013; Sullivan *et al.* 2017). Most of Gabon's AGC is stored in large trees: trees ≥50 cm DBH account for 6.6% of stems and 51.3% of AGC and trees ≥70 cm DBH account for 2.3% of trees and 30.6% of AGC. Here, we also establish baseline estimates of old growth (166.6 Mg C ha^{-1}), concession (171.3 Mg C ha^{-1}), and secondary (96.6 Mg C ha^{-1}) forests (Table 1). Note that mean AGC and AGC in primary *terra firma*, closed canopy forest (168.6 Mg C ha^{-1}; 95% CI [151.1, 186.1]) in Gabon are significantly lower than values reported for African humid tropical forests

For Peer Review

from research plots (202 Mg C ha^{-1}; Lewis *et al.* 2013a). This difference is likely attributable to the NRI's probabilistic sampling design (Fig. 1) that captures a combination of intact and partially disturbed forests, unlike research plots concentrated in undisturbed, old growth forest (e.g. Xu *et al.* 2017).

Despite being one of the world's most forested countries, with a very low population density and deforestation rate, in Gabon human activities are the dominant drivers of variation in AGC and numbers of large trees. Of environmental variables, only soil fertility positively influenced AGC and no variables strongly affected numbers of large trees; whereas climate and soils contributed importantly to variation in mean basal area, tree height, wood density, and stem density. In many tropical countries, tackling climate change by reducing carbon emissions depends on working at the deforestation front and promoting reforestation. In Gabon, conservation of its stable, majestic forests ought to be a priority, while also carefully managing high carbon, degraded forests and promoting regeneration of secondary forests. Protecting forests that are not already significantly disturbed and that contain abundant large trees can conserve carbon, biodiversity, and ecosystem services (Funk et al. 2019).

Gabon's NRI is one of the most rigorous national inventories of tropical forest to date. The inventory employs internationally recognized data collection methods, relatively large plots to increase precision (Chave *et al.* 2004), and samples forest and disturbance types relative to their representation while avoiding the 'majestic forest' bias. With funding from the Central African Forest Initiative (CAFI), additional sites are being added to the NRI and the sampling sites reported here are being remeasured to monitor carbon dynamics over time. The NRI data are important nationally and regionally for reporting on greenhouse gas emissions. Nations that are parties to the United Nations Framework Convention on Climate Change (UNFCCC) must report on emissions and removals for climate change mitigation efforts, and the reducing emissions from deforestation and forest degradation (REDD+) policy framework will require establishment of reference emission levels for comparison against future emissions measured by a monitoring, reporting and verification system (MRV). With limited forest monitoring in the tropics, many countries rely on default values in IPCC guidelines (IPCC 2006) to estimate emissions, rather than country-specific data (Tier 2) or higher-level methods like repeated measurements of permanent plots (Tier 3). Gabon's NRI is on track to achieve Tier 3 reporting and contribute to improving IPCC default rates (Suarez *et al.* 2019). By making its data openly accessible, Gabon could advance the development of regional and global policies to fight climate change.

Importance of Large Trees to AGC

In Gabon, like other tropical forests, large trees are the major constituents of live AGC. Intact African forests are characterized by their large trees (Feldpausch *et al.* 2012; Lewis *et al.* 2013), and we

For Peer Review

found the largest 5% of trees store 50% of AGC on average similar to Central Africa in general (Bastin *et al.* 2015). However, the proportional contribution of large trees to AGC varied with disturbance type: secondary forest, with a lower average AGC, accumulates AGC at a faster rate from large trees than primary and concession forest. Loss of the largest trees drastically changes forest structure and diameter distributions; thus understanding the relative importance of large trees to AGC in different forest types could help characterize forest degradation, which accounts for a large fraction of carbon loss worldwide (Pan *et al.* 2013). Large tree biomass in Gabon is also correlated with high densities of coarse woody debris (Carlson *et al.* 2017) and large liana biomass (Poulsen *et al.* 2017); thus, the loss of large trees could affect multiple pools of carbon.

Large trees are typically defined as having diameters ≥70 cm, but Meyer *et al.* (2018) determined that a threshold of >50 cm DBH was more reliable for quantifying the number and distribution of large trees in old-growth Neotropical forests. Rethinking the definition of large trees could have several advantages. First, defining only 2.3% of stems as 'large' seems extreme. In Gabon, trees ≥50 cm make up 6.6% of all stems and 51.3% of AGC – still a small proportion of trees but ~20% more in measured AGC. If 'large trees' were protected by law in industrial agricultural fields, for example, more carbon could be preserved with the conservation of only 4.3% more stems. Second, in our study, basal area and tree height explain AGC; therefore, relaxing the definition of 'large' might capture some smaller diameter, tall trees that contribute to AGC. Third, in Gabon selective logging starts at a minimum cutting diameter of 40 cm for *Diospyros crassiflora*, with minimum harvest diameters of 60-90 cm for 60 species and 70 cm for all others (Ministère des eaux et forêts 2014). Accounting for large trees of ≥50 cm DBH would more thoroughly capture the effects of logging.

Drivers of Large Trees and AGC

Precipitation, soil types and ecosystems vary spatially across Gabon, yet our results indicate that anthropogenic disturbance (disturbance type and distance from villages) is the primary driver of numbers of large trees and AGC and strongly influences other stand variables (Figure 6). Soil fertility was the only environmental variable to influence AGC. Like previous studies, stand variables including number of large trees, basal area and tree height explained most of the variation in plot-level AGC. Interestingly, basal-area weighted wood density also explained a relatively high level of variation in AGC compared to other studies (Lewis *et al.* 2013; Bastin *et al.* 2018). Florist species composition may, therefore, be an important factor influencing AGC in Gabon. Wood density was marginally correlated with distance from villages (r = 0.184, df = 102, p = 0.06), suggesting a floristic gradient of pioneer to old-growth species explained by distance from the road network.

For Peer Review

Although environmental variables exerted weak control over large trees and AGC, climate, soil, and topography influenced stand variables that explain most of the spatial variation in AGC. Environmental variables can strongly affect stand variables while explaining little overall variation in AGC because they covary negatively in their responses to climate, soils, and topography (Baraloto *et al.* 2011). In fact, the environmental variables considered here often differentially affected forest stand variables. For example, basal area and number of trees increased with slope, whereas tree heights declined (Figure 6). Because stand variables are components of AGC, identifying the drivers of individual stand variables is important for understanding the mechanisms of temporal-spatial variation in AGC (Bastin *et al.* 2018).

In Gabon, secondary forests have significantly lower carbon stocks than primary forests, but with an average of 96.6 Mg C ha^{-1}, they are on the high side of AGC estimates from other tropical countries like Costa Rica (82.2 Mg C ha^{-1}) and Sierra Leone, where old fallows with residual trees have 80 Mg C ha^{-1} (Fonseca *et al.* 2011; Cuni Sanchez & Lindsell 2017). In Cameroon, forest fallows contain 50% of the carbon stocks of an old-growth forest (Njomgang *et al.* 2011), whereas in Gabon they hold 63%. Gabon's secondary forests have important conservation value because of their relatively high carbon stocks, as well as for their carbon sequestration potential: secondary forests can uptake carbon 11 times as fast as old growth forests (Poorter *et al.* 2016).

Regeneration of secondary and disturbed forests to their natural state can sequester more carbon than agroforestry and plantations (Lewis *et al.* 2019); thus, highly forested, developing countries like Gabon must carefully balance development and climate change mitigation. In the Congo Basin, small-scale, nonmechanized forest clearing for agriculture doubled between 2000 and 2014 (Tyukavina *et al.* 2018). Although this type of slash-and-burn farming contributes less to forest clearing in Gabon than other countries, it undoubtedly explains increasing AGC with distance from villages. Slash-and-burn farming converts forest to fields every 3-5 years to maintain productivity. Reducing the expansion of secondary forest, therefore, will require crops with longer rotation times, application of expensive fertilizers, or a transition to high intensity agriculture. Currently, industrial production of oil palm and rubber makes up just 0.8% of the land area in Gabon (Tyukavina *et al.* 2018), but this is projected to increase as the Congo Basin goes through a new wave of agroindustry development (Feintrenie 2014; Austin *et al.* 2017). Most secondary forests in Gabon surpass the carbon threshold (75 Mg C ha^{-1}) above which the High Carbon Stock approach discourages development (HCS Technical Committee 2015), indicating that plantation siting must consider AGC, and offsets or other measures may be required to mitigate planned deforestation (Burton *et al.* 2017).

For Peer Review

Selective logging, Gabon's primary land use activity, constitutes 61.6% of forest loss (Tyukavina *et al.* 2018). Concession forest contains slightly higher AGC than primary forest even though significant carbon losses follow conventional and reduced impact logging (Medjibe *et al.* 2013). Excluding savanna, swamps and flooded forests, where logging would not occur, primary forests store 166.6 Mg C ha^{-1} on average, nearly the same as concession forest (171.3 Mg C ha^{-1}). High AGC in concession forests is likely a result of grouping all sites that occurred in timber concessions together, whether they had been logged or not, or possibly by landscape-level high grading, where forests with the largest trees are selected for timber harvest. Low harvest intensity in Central Africa, rarely exceeding 10-13 m^3 per hectare or 4-8% of standing timber volume (Karsenty 2016), might also allow logged forests to recover rapidly (Rutishauser *et al.* 2015). If our results hold up under additional study, they argue for including sustainable forestry in programs like REDD+.

Protected areas worldwide store 15.2% of global terrestrial carbon stocks and reduce carbon emissions (Bebber & Butt 2017). Gabon's national parks and reserves, 18.4% of the country's landmass, store significantly higher densities of AGC than forests outside of parks. The 49,256 km^2 of forested lands in parks and reserves store approximately 0.84 Gt C or 25.4% of AGC. Gabon's protected areas, therefore, are an important component of its climate mitigation strategy. At the same time, most terrestrial carbon (2.47 Gt C) lies outside of protected areas and requires concerted management as the government grows its agricultural sector (Austin *et al.* 2017). Two areas of high carbon density occur along the southwestern coast and in the northeastern part of the country. Both areas include parks separated by logging concessions. With careful management, these concessions could contribute to Gabon's timber industry, capture carbon through forest regrowth, and conserve biodiversity.

Conclusion

Based on a rigorous national inventory of forestlands in Gabon, we demonstrate that Central African forests can hold high densities of AGC in secondary and concession forests, as well as old-growth forests. Combatting climate change, therefore, will require a combined approach that includes measures for conserving, managing, and regenerating tropical forests. The international community proposes to pay developing nations to reduce greenhouse gas emissions from deforestation and forest degradation (REDD+). Additional policies will be necessary. Agricultural development or other activities that necessitate deforestation should only occur in secondary forests with low AGC. Importantly, international mechanisms should also include provisions for promoting the permanence of stable, intact old growth forests like those in Gabon (Funk *et al.* 2019). Similar attention should be given to logging concessions in carbon dense forests that represent a large proportion of remaining Central African

For Peer Review

forests. Protecting forests that are not already significantly disturbed will require considerable international financial assistance to promote low emissions development and policies such as country-wide forest certification. The preservation of the world's large primary forests will conserve carbon, biodiversity, and ecosystem services now, and avoid the rush to save the remnants of diminished, low carbon secondary forest later.

DATA AVAILABILITY STATEMENT

The data are subject to third party restrictions. The data that support the findings of this study are available from Le Ministère des Eaux, de la Forest, de la Mer, de l'Environnement. Restrictions apply to the availability of these data, which were used under license for this study. Data are available from the corresponding author with the permission of Le Ministère des Eaux, de la Forest, de la Mer, de l'Environnement.

For Peer Review

Austin, K.G., Lee, M.E., Clark, C., Forester, B.R., Urban, D.L., White, L., *et al.* (2017). An assessment of high carbon stock and high conservation value approaches to sustainable oil palm cultivation in Gabon. *Environ. Res. Lett.*, 12, 014005.

Banin, L., Feldpausch, T.R., Phillips, O.L., Baker, T.R., Lloyd, J., Affum-Baffoe, K., *et al.* (2012). What controls tropical forest architecture? Testing environmental, structural and floristic drivers. *Glob. Ecol. Biogeogr.*, 21, 1179–1190.

Baraloto, C., Rabaud, S., Molto, Q., Blanc, L., Fortunel, C., Hérault, B., *et al.* (2011). Disentangling stand and environmental correlates of aboveground biomass in Amazonian forests. *Glob. Chang. Biol.*, 17, 2677–2688.

Barton, K. (2019). Package ‘ MuMIn’: Multi-Model Inference.

Bastin, J.F., Barbier, N., Réjou-Méchain, M., Fayolle, A., Gourlet-Fleury, S., Maniatis, D., *et al.* (2015). Seeing Central African forests through their largest trees. *Sci. Rep.*, 5, 1–8.

Bastin, J.F., Rutishauser, E., Kellner, J.R., Saatchi, S., Pélissier, R., Hérault, B., *et al.* (2018). Pan-tropical prediction of forest structure from the largest trees. *Glob. Ecol. Biogeogr.*

Bayol, N., Demarquez, B., Wasseige, C. De, Eba, R., Fisher, J., Nasi, R., *et al.* (2012). Forest management and the timber sector in Central Africa. In: *The forests of the Congo Basin: state of the Forest 2010* (eds. Wasseige, C. de, Marcken, P.J. De, Bayol, N., Hiol, F.H., Mayaux, P., Desclée, B., et al.). Publications Office of the European Union, Luxembourg, pp. 43–62.

Bebber, D.P. & Butt, N. (2017). Tropical protected areas reduced deforestation carbon emissions by one third from 2000-2012. *Sci. Rep.*, 7, 1–8.

Beirne, C., Miao, Z., Nuñez, C.L., Medjibe, V.P., Saatchi, S., White, L.J.T., *et al.* (2019). Landscape-level validation of allometric relationships for carbon stock estimation reveals bias driven by soil type. *Ecol. Appl.*, 29, e01987.

Berenguer, E., Ferreira, J., Gardner, T.A., Aragão, L.E.O.C., De Camargo, P.B., Cerri, C.E., *et al.* (2014). A large-scale field assessment of carbon stocks in human-modified tropical forests. *Glob. Chang. Biol.*, 20, 3713–3726.

Born, C., Alvarez, N., McKey, D., Ossari, S., Wickings, E.J., Hossaert-Mckey, M., *et al.* (2011). Insights into the biogeographical history of the Lower Guinea Forest Domain: Evidence for the role of refugia in the intraspecific differentiation of Aucoumea klaineana. *Mol. Ecol.*, 20, 131–142.

Burton, M.E.H., Poulsen, J.R., Lee, M.E., Medjibe, V.P., Stewart, C.G., Venkataraman, A., *et al.* (2017). Reducing Carbon Emissions from Forest Conversion for Oil Palm Agriculture in Gabon. *Conserv. Lett.*, 10, 297–307.

For Peer Review

Cade, B.S. (2015). Model averaging and muddled multimodel inferences. *Ecology*, 96, 2370–2382.

Carlson, B.S., Koerner, S.E., Medjibe, V.P., White, L.J.T. & Poulsen, J.R. (2017). Deadwood stocks increase with selective logging and large tree frequency in Gabon. *Glob. Chang. Biol.*, 23, 1648–1660.

Chave, J., Condit, R., Aguilar, S., Hernandez, A., Lao, S. & Perez, R. (2004). Error propagation and scaling for tropical forest biomass estimates. *Philos. Trans. R. Soc. B Biol. Sci.*, 359, 409–420.

Chave, J., Muller-landau, H.C., Baker, T.R., Easdale, T. a & Webb, C.O. (2014a). Regional and Phylogenetic Variation of Wood Density across 2456 Neotropical Tree Species, 16, 2356–2367.

Chave, J., Réjou-Méchain, M., Búrquez, A., Chidumayo, E., Colgan, M.S., Delitti, W.B.C., *et al.* (2014b). Improved allometric models to estimate the aboveground biomass of tropical trees. *Glob. Chang. Biol.*, 20, 3177–3190.

Cuni Sanchez, A. & Lindsell, J.A. (2017). The role of remnant trees in carbon sequestration, vegetation structure and tree diversity of early succession regrowing fallows in eastern Sierra Leone. *Afr. J. Ecol.*, 55, 188–197.

FAO. (2002). *Terrastat, global land resources GIS models and data- bases for poverty and food insecurity mapping.*

Feintrenie, L. (2014). Agro-industrial plantations in Central Africa, risks and opportunities. *Biodivers. Conserv.*, 23, 1577–1589.

Feldpausch, T.R., Lloyd, J., Lewis, S.L., Brienen, R.J.W., Gloor, M., Monteagudo Mendoza, A., *et al.* (2012). Tree height integrated into pantropical forest biomass estimates. *Biogeosciences*, 9, 3381–3403.

Fonseca, W., Rey Benayas, J.M. & Alice, F.E. (2011). Carbon accumulation in the biomass and soil of different aged secondary forests in the humid tropics of Costa Rica. *For. Ecol. Manage.*, 262, 1400–1408.

Forêt Ressources Management. (2018). *Vision stratégique et industrialisation de la filière bois dans les 6 pays du Bassin du Congo: Horizon 2030*. Montpelier, France.

Funk, J.M., Aguilar-Amuchastegui, N., Baldwin-Cantello, W., Busch, J., Chuvasov, E., Evans, T., *et al.* (2019). Securing the climate benefits of stable forests. *Clim. Policy*, 0, 1–16.

Galipaud, M., Gillingham, M.A.F. & Dechaume-Moncharmont, F.X. (2017). A farewell to the sum of Akaike weights: The benefits of alternative metrics for variable importance estimations in model selection. *Methods Ecol. Evol.*, 8, 1668–1678.

Gibbs, H.K., Ruesch, A.S., Achard, F., Clayton, M.K., Holmgren, P., Ramankutty, N., *et al.* (2010).

For Peer Review

Tropical forests were the primary sources of new agricultural land in the 1980s and 1990s. *Proc. Natl. Acad. Sci.*, 107, 16732–16737.

HCS Technical Committee. (2015). *The High Carbon Stock Science Study: Independent Report from the Technical Committee*.

Hijmans, R.J., Cameron, S.E., Parra, J.L., Jones, P.G. & Jarvis, A. (2005). Very high resolution interpolated climate surfaces for global land areas. *Int. J. Climatol.*, 25, 1965–1978.

IPCC. (2006). 2006 IPCC Guidelines for National Greenhouse Inventories – A primer, Prepared by the National Greenhouse Gas Inventories Programme, Eggleston H.S., Miwa K., Srivastava N. and Tanabe K. *Iges*, 20.

Karsenty, A. (2016). *The contemporary forest concessions in West and Central Africa: chronicle of a foretold decline? For. Policy Institutions Work. Pap.* Rome.

Lescuyer, G., Cerutti, P., Manguiengha, S.N. & bi Ndong, L.B. (2011). *The domestic market for small-scale chainsaw milling in Cameroon : present situation, opportunities and challenges*. Occasional. Center for International Forestry Research, Bogor, Indonesia.

Lewis, S.L., Edwards, D.P. & Galbraith, D. (2015). Increasing human dominance of tropical forests. *Science (80-.)*., 349, 827–832.

Lewis, S.L., Sonke, B., Sunderland, T., Begne, S.K., Lopez-Gonzalez, G., van der Heijden, G.M.F., *et al.* (2013). Above-ground biomass and structure of 260 African tropical forests. *Philos. Trans. R. Soc. B Biol. Sci.*, 368, 20120295–20120295.

Lewis, S.L., Wheeler, C.E., Mitchard, E.T.A. & Koch, A. (2019). Restoring natural forests is the best way to remove atmospheric carbon. *Nature*, 568, 25–28.

Lindenmayer, D.B., Laurance, W.F. & Franklin, J.F. (2012). Global decline in large old trees. *Science (80-.)*., 338, 1305–1306.

Malhi, Y., Wood, D., Baker, T.R., Wright, J., Phillips, O.L., Cochrane, T., *et al.* (2006). The regional variation of aboveground live biomass in old-growth Amazonian forests. *Glob. Chang. Biol.*, 12, 1107–1138.

McMahon, S.M., Parker, G.G. & Miller, D.R. (2010). Evidence for a recent increase in forest growth. *Proc. Natl. Acad. Sci.*, 107, 3611–3615.

Medjibe, V.P., Putz, F.E. & Romero, C. (2013). Certified and uncertified logging concessions compared in Gabon: Changes in stand structure, tree species, and biomass. *Environ. Manage.*, 51, 524–540.

Meyer, V., Saatchi, S., Clark, D.B., Keller, M., Vincent, G., Ferraz, A., *et al.* (2018). Canopy area of large trees explains aboveground biomass variations across neotropical forest landscapes.

For Peer Review

Biogeosciences, 15, 3377–3390.

Ministère des eaux et forêts. (2014). Code Forestier de la République Gabonaise.

Ngomanda, A., Engone Obiang, N.L., Lebamba, J., Moundounga Mavouroulou, Q., Gomat, H., Mankou, G.S., *et al.* (2014). Site-specific versus pantropical allometric equations: Which option to estimate the biomass of a moist central African forest? *For. Ecol. Manage.*, 312, 1–9.

Van Nieuwstadt, M.G.L. & Sheil, D. (2005). Drought, fire and tree survival in a Borneo rain forest, East Kalimantan, Indonesia. *J. Ecol.*, 191–201.

Njomgang, R., Yemefack, M., Nounamo, L., Moukam†, A. & Kotto-Same†, J. (2011). Dynamics of Shifting Agricultural-Systems and Organic Carbon Sequestration in Southern Cameroon. *Tropicultura*, 29, 176–182.

Pan, Y., Birdsey, R.A., Phillips, O.L. & Jackson, R.B. (2013). The Structure, Distribution, and Biomass of the World's Forests. *Annu. Rev. Ecol. Evol. Syst.*, 44, 593–622.

Poorter, L., Bongers, F., Aide, T.M., Almeyda Zambrano, A.M., Balvanera, P., Becknell, J.M., *et al.* (2016). Biomass resilience of Neotropical secondary forests. *Nature*, 530, 211–214.

Poulsen, J.R., Koerner, S.E., Miao, Z., Medjibe, V.P., Banak, L.N. & White, L.J.T. (2017). Forest structure determines the abundance and distribution of large lianas in Gabon. *Glob. Ecol. Biogeogr.*, 26, 472–485.

Quesada, C.A., Phillips, O.L., Schwarz, M., Czimczik, C.I., Baker, T.R., Patiño, S., *et al.* (2012). Basin-wide variations in Amazon forest structure and function are mediated by both soils and climate. *Biogeosciences*, 9, 2203–2246.

R Core Team. (2018). R: A language and environment for statistical computing.

Rutishauser, E., Hérault, B., Baraloto, C., Blanc, L., Descroix, L., Sotta, E.D., *et al.* (2015). Rapid tree carbon stock recovery in managed Amazonian forests. *Curr. Biol.*, 25, R787–R788.

Saatchi, S.S., Harris, N.L., Brown, S., Lefsky, M., Mitchard, E.T.A., Salasf, W., *et al.* (2011). Benchmark map of forest carbon stocks in tropical regions across three continents. *Proc. Natl. Acad. Sci.*, 108, 9899–9904.

Sannier, C., McRoberts, R.E., Fichet, L.V. & Makaga, E.M.K. (2014). Using the regression estimator with landsat data to estimate proportion forest cover and net proportion deforestation in gabon. *Remote Sens. Environ.*, 151, 138–148.

Slik, J.W.F. (2004). El Niño droughts and their effects on tree species composition and diversity in tropical rain forests. *Oecologia*, 141, 114–120.

Slik, J.W.F., Aiba, S.I., Brearley, F.Q., Cannon, C.H., Forshed, O., Kitayama, K., *et al.* (2010).

For Peer Review

Environmental correlates of tree biomass, basal area, wood specific gravity and stem density gradients in Borneo's tropical forests. *Glob. Ecol. Biogeogr.*, 19, 50–60.

Slik, J.W.F., Paoli, G., Mcguire, K., Amaral, I., Barroso, J., Bastian, M., *et al.* (2013). Large trees drive forest aboveground biomass variation in moist lowland forests across the tropics. *Glob. Ecol. Biogeogr.*, 22, 1261–1271.

ter Steege, H., Pitman, N.C.A., Sabatier, D., Baraloto, C., Salomão, R.P., Guevara, J.E., *et al.* (2013). Hyperdominance in the Amazonian tree flora. *Science (80-.).*, 342, 1243092.

Stegen, J.C., Swenson, N.G., Enquist, B.J., White, E.P., Phillips, O.L., Jørgensen, P.M., *et al.* (2011). Variation in above-ground forest biomass across broad climatic gradients. *Glob. Ecol. Biogeogr.*, 20, 744–754.

Suarez, D.R., Phillips, O.L., Rozendaal, D.M.A., Sy, V. De, Dávila, E.A., Teixeira, K.A., *et al.* (2019). Estimating aboveground net biomass change for tropical and subtropical forests : Refinement of IPCC default rates using forest plot data. *Glob. Chang. Biol.*, 25, 3609–3624.

Sullivan, M.J.P., Lewis, S.L., Hubau, W., Qie, L., Baker, T.R., Banin, L.F., *et al.* (2018). Field methods for sampling tree height for tropical forest biomass estimation. *Methods Ecol. Evol.*, 9, 1179–1189.

Sullivan, M.J.P., Talbot, J., Lewis, S.L., Phillips, O.L., Qie, L., Begne, S.K., *et al.* (2017). Diversity and carbon storage across the tropical forest biome. *Sci. Rep.*, 7, 1–12.

Theobald, D.M., Stevens, D.L., White, D., Urquhart, N.S., Olsen, A.R. & Norman, J.B. (2007). Using GIS to generate spatially balanced random survey designs for natural resource applications. *Environ. Manage.*, 40, 134–146.

Thomas, S.C. & Martin, A.R. (2012). Carbon content of tree tissues: A synthesis. *Forests*, 3, 332–352.

Tyukavina, A., Hansen, M.C., Potapov, P., Parker, D., Okpa, C., Stehman, S. V., *et al.* (2018). Congo Basin forest loss dominated by increasing smallholder clearing. *Sci. Adv.*, 4, eaat2993.

Wade, A.M., Richter, D.D., Medjibe, V.P., Bacon, A.R., Heine, P.R., White, L.J.T., *et al.* (2019). Estimates and determinants of stocks of deep soil carbon in Gabon, Central Africa. *Geoderma*, 341, 236–248.

World Resources Institute. (2017). *Congo Basin Forest Atlases*.

Xu, L., Saatchi, S.S., Shapiro, A., Meyer, V., Ferraz, A., Yang, Y., *et al.* (2017). Spatial Distribution of Carbon Stored in Forests of the Democratic Republic of Congo. *Sci. Rep.*, 7, 1–13.

Yang, Y., Saatchi, S.S., Xu, L., Yu, Y., Lefsky, M.A., White, L., *et al.* (2016). Abiotic controls on macroscale variations of humid tropical forest height. *Remote Sens.*, 8, 1–18.

Zanne, A.E., Lopez-Gonzalez, G., Coomes, D.A., Ilic, J., Jansen, S., Lewis, S.L., *et al.* (2009). Data from: Towards a worldwide wood economics spectrum. *Dryad Digit. Repos.*

For Peer Review

Zhu, K., Zhang, J., Niu, S., Chu, C. & Luo, Y. (2018). Limits to growth of forest biomass carbon sink under climate change. *Nat. Commun.*, 9.

For Peer Review

Table 1. Summary statistics of Gabon's NRI, including sites consisting of one 1-ha plot and four 0.16-ha satellite plots (see Methods, 16 sites have fewer than four satellite plots) and 1-ha plots for comparison with other studies. AGC is calculated with Chave et al.'s (2014) pantropical equation, except Gabon* is calculated using the Gabon-specific equation that estimated AGC as 26% lower (range = 6.2-48.3%).

Variable	NRI Sites Mean ha^{-1} [95% CI]	NRI 1-ha Plots Mean ha^{-1} [95% CI]
No. sites	104	104
Area, ha	164.3	104
No. plots by size, ha	377 0.16-ha, 104 1-ha	104 1-ha
No. trees ha^{-1}	407.5 [387.7, 427.2]	415.8 [393.6, 438.0]
DBH (D), cm	23.3 [22.8, 23.8]	23.5 [22.9, 24.1]
DBH max, cm	125.2 [118.3, 132.1]	117.6 [111.2, 123.9]
Wood density (ρ), g cm^{3}	0.628 [0.612, 0.644]	0.630 [0.613, 0.647]
Height (H), m	20.4 [19.4, 21.5]	20.5 [19.5, 21.6]
Height max, m	39.7 [37.9, 41.4]	38.9 [37.2, 40.7]
BA, m^{2} ha^{-1}	25.3 [23.8, 26.7]	26.0 [24.5, 27.6]
Aboveground carbon, Mg ha^{1}		
Gabon	141.7 [130.1, 153.3]	146.4 [133.6, 159.3]
Gabon*	112.3 [103.1, 121.6]	116.1 [105.9, 126.3]
Primary forest (n = 43)	151.9 [134.8, 169.0]	156.6 [138.1, 175.2]
Primary, *terra firma* forest (n = 27)	166.6 [150.2, 183.1]	168.6 [151.1, 186.1]
Concession forest (n = 31)	171.3 [154.8, 187.7]	178.5 [158.5, 198.4]
Secondary forest (n = 30)	96.6 [77.0, 116.2]	98.7 [77.3, 120.0]
Parks/reserves (n = 21)	170.9 [139.3, 202.4]	174.7 [140.1, 209.4]
Non-park/reserve forests (n = 83)	134.3 [122.3, 146.4]	139.3 [125.8, 152.7]
Central forest (n = 51)	144.9 [130.9, 159.0]	148.6 [132.4, 164.7]
Coastal forest (n = 29)	152.8 [126.2, 179.3]	157.7 [127.9, 187.4]
Northeast forest (n = 15)	155.1 [132.3, 178.0]	161.9 [137.1, 186.7]
Savanna forest (n = 9)	65.6 [23.5, 107.7]	72.1 [28.2, 116.1]

For Peer Review

Figure 1. (a) Map of Gabon (grey polygon) within Africa. (b) Map of national roads (yellow lines) and national parks and presidential reserves (black polygons). (c) Map of Gabon overlain with a 50 x 50 km grid, showing the systematic, random location of forest plots (black symbols). (d) Map of Gabon with major ecosystems (yellow = coastal forest, blue = central forest, brown = northeastern forest, red = savanna). (e) Location of plot sites, colored by disturbance type (yellow = primary forest, blue = concession forest, red = secondary forest).

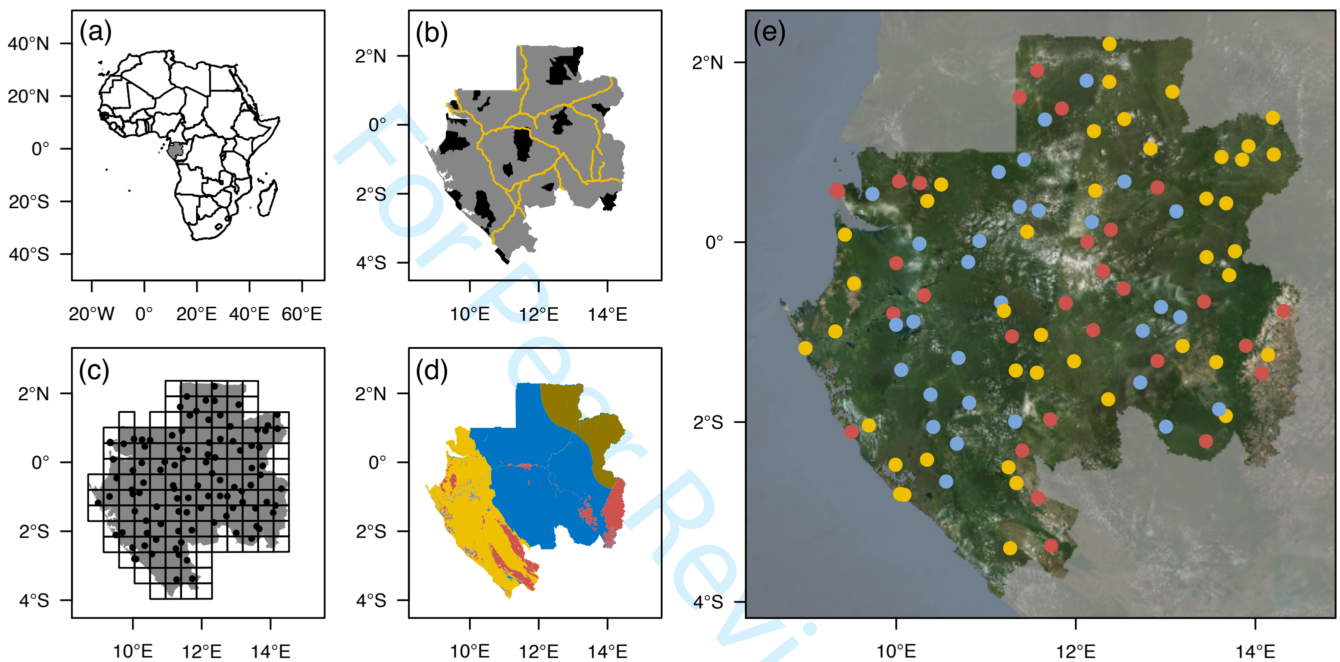

For Peer Review

Figure 2. Aboveground carbon for 104 NRI sites plotted against (a) mean basal area ($F_{1,102}$ = 232.8, p < 0.001, R^2 = 0.692); (b) tree height ($F_{1,102}$ = 115, p < 0.001, R^2 = 0.525); (c) wood mass density ($F_{1,102}$ = 74.04, p < 0.001, R^2 = 0.415), (d) stem density ($F_{1,102}$ = 11.48, p = 0.001, R^2 = 0.092), (e) total AGC of large trees at the site ($F_{2,101}$ = 138.6, p < 0.001, R^2 = 0.728); and (f) number of large trees ($F_{1,101}$ = 132.8, p < 0.001, R^2 = 0.561). Black lines represent the best-fit regression line for all disturbance types with their 95% confidence intervals (shading), and colored lines are slopes from analyses of covariance testing the interaction between disturbance type (yellow = primary, blue = concession, red = secondary) and stand variables on AGC.

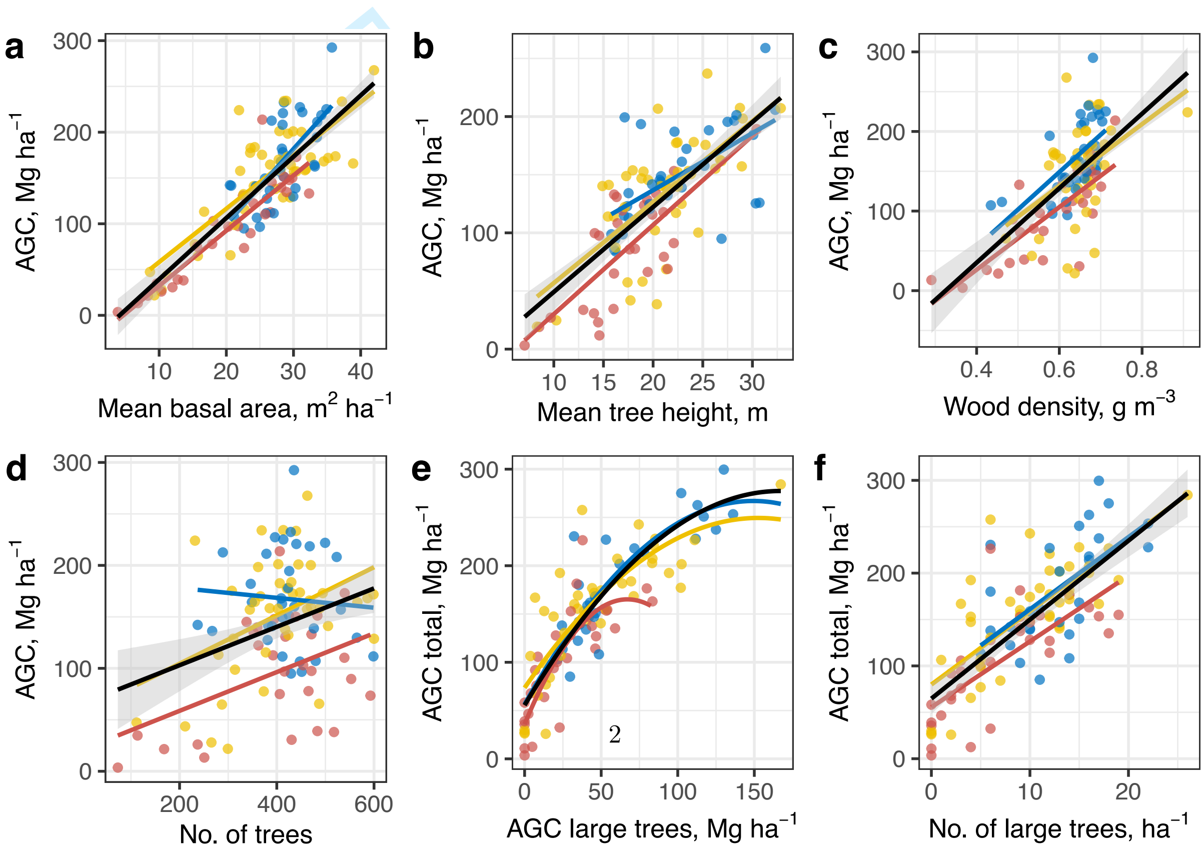

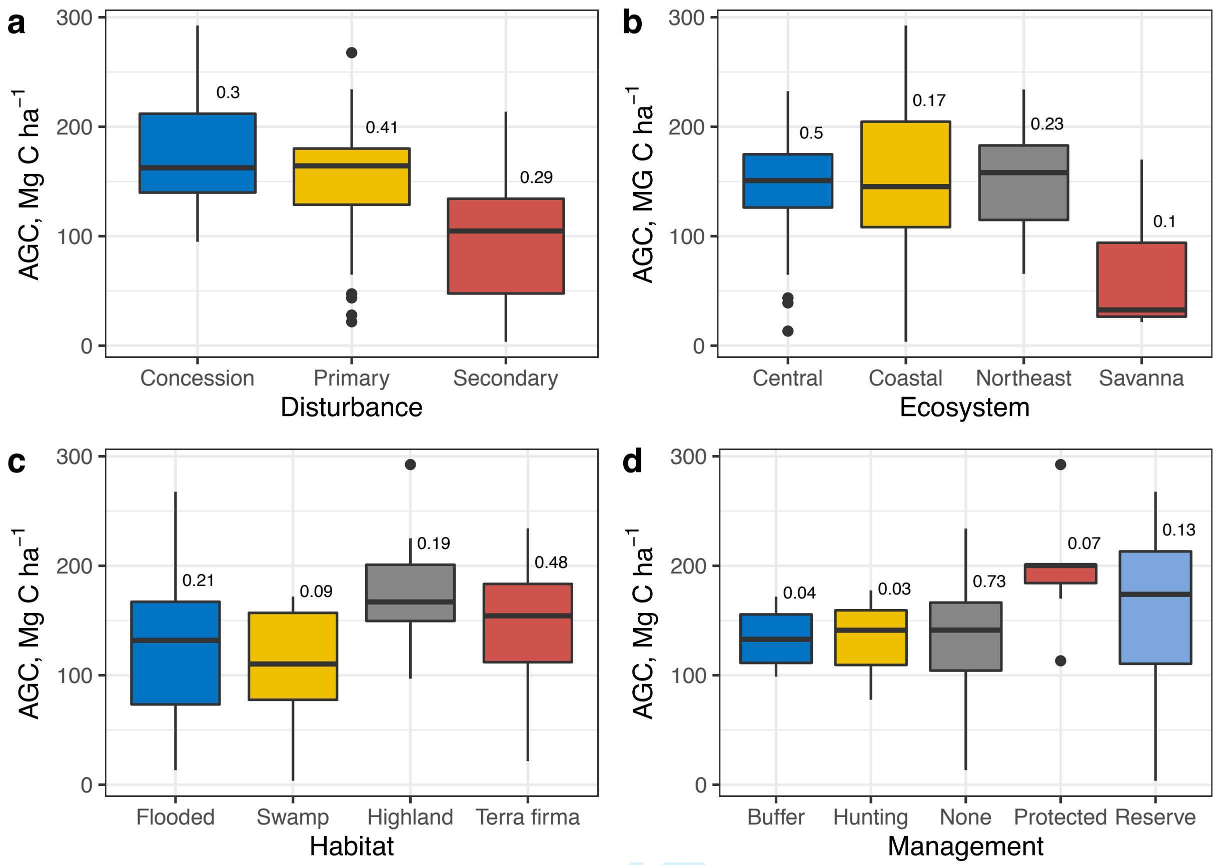

Figure 3. AGC of NRI sites by (a) Disturbance type: plots in secondary forest have significantly lower AGC than primary and concession forest ($F_{2,101}$ = 16.5, p < 0.001); (b) Ecosystem: plots in savanna hold significantly lower AGC than all other ecosystem types ($F_{3,100}$ = 8.0, p < 0.001); (c) Forest type: highland plots contain significantly higher AGC than swamps and flooded forests ($F_{3,97}$ = 4.04, p = 0.009), and (d) Management: plots in protected areas contain significantly higher AGC than areas with no management (F = $2.1_{4,99}$, p = 0.0865), and plots in protected and reserve areas contain significantly higher AGC than other management types (F = $6.47_{1,102}$, p = 0.0125). The number to the right of each boxplot is the proportion of all sites belonging to that category (e.g. 30% of sites were in concession forests).

Figure 4. Extrapolation maps showing the predicted distribution of (a) aboveground carbon, Mg ha^{-1}; (b) mean basal area, m^2 ha^{-1}; (c) tree height, m; (d) wood density, g cm^{-3}; (e) numbers of stems, ha^{-1}; and, (f) numbers of large trees (stems ≥70 cm DBH) in field plots across Gabon. The color scale for each map is mean-centered so that white areas are average, shades of orange are above and shades of purple are below average. Forests with high carbon and tall trees occur largely along the coast and northeastern section of Gabon. Forests with high numbers of large trees also occur in the northeast, which was opened up relatively late to industrial logging, agriculture, and mining compared to the western and southern sections of the country. Gabon's high carbon forests are also relatively isolated from the national road network along which most villages lie (Figure 1).

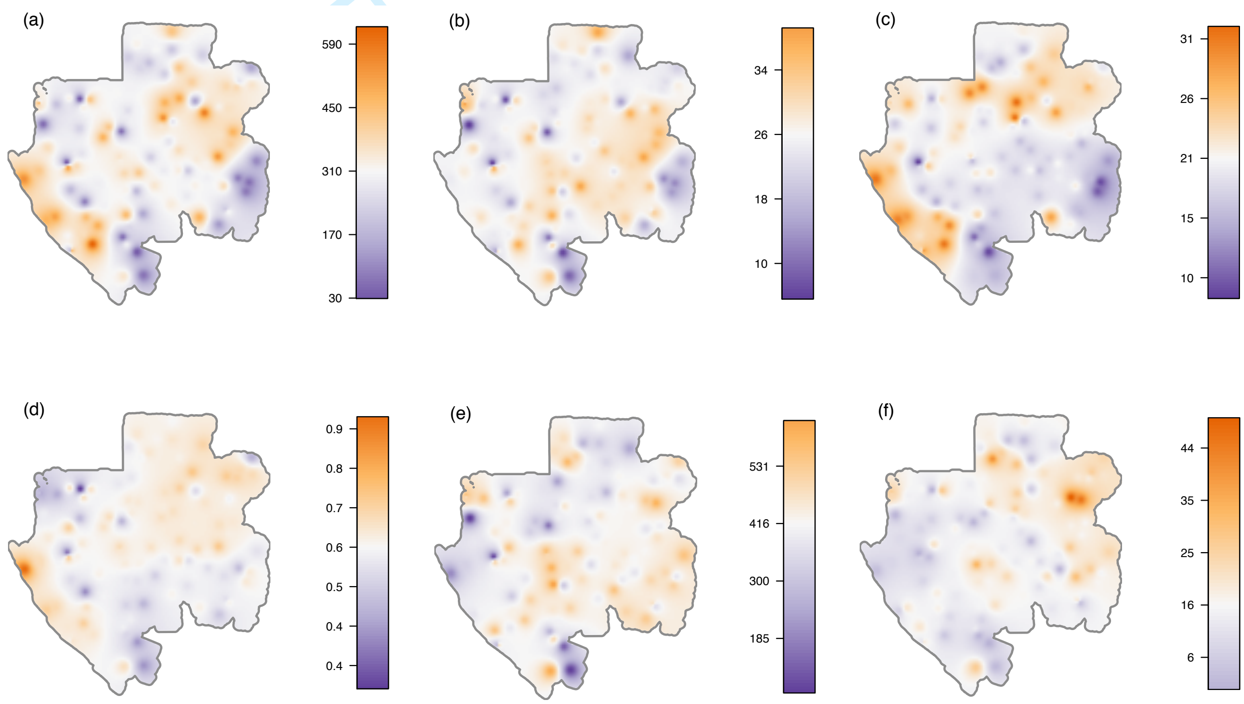

Figure 5. (a) The mean proportion of total AGC represented by the cumulative addition of the largest trees. Black dashed line shows all data; colored lines depict each disturbance type (yellow = primary forest, blue = concession forest, red = secondary forest). (inset) AGC of the largest trees versus the total AGC of 1-ha plots for each disturbance type and all disturbance types combined (black dashed line). (b) Fits of models predicting variation in total AGC explained by the cumulative addition of large trees: different forest types have different accumulation curves.

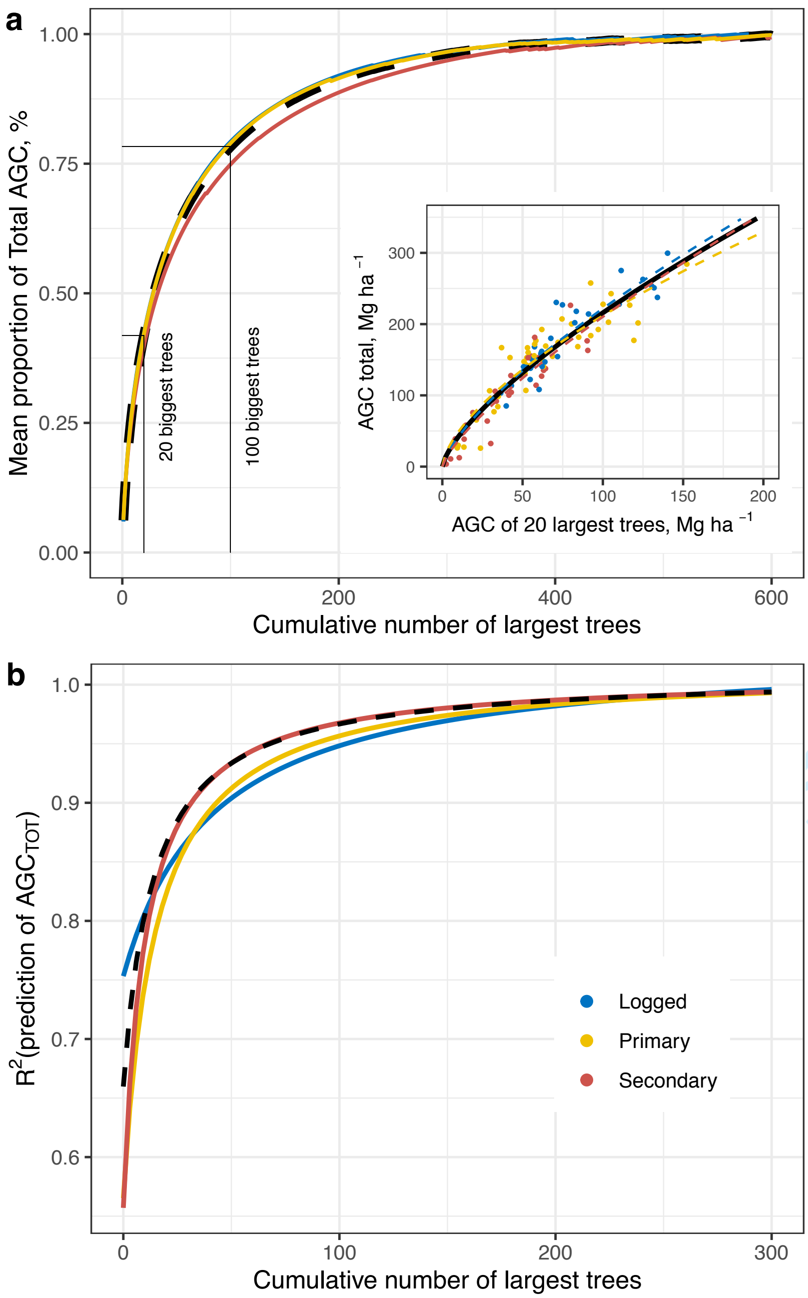

Figure 6. Relative effects of independent variables on stand variables, including (a) AGC, Mg ha^{-1}; (b) basal area, m^2 ha^{-1}; (c) tree height, m; (d) wood density g cm^{-3}; (e) number of trees ha^{-1}; and, (f) number of large trees ha^{-1}. The size of the symbols represents model support for the effects. The position of the symbols on the x-axis represents the relative effect size of the standardized coefficients, calculated as $E_{Rel,i} = E_i / \sum E_i$. Independent variables include distance from villages (Vill), slope (Slope), soil fertility (Sfert), soil drainage (Sdrain), soil depth (Sdepth), savanna (Savanna), seasonality of precipitation (Pseas), total annual precipitation (Precip), precipitation in the driest quarter (Pdryq), longitude (Lon), latitude (Lat), secondary forest (DT-Sec), and elevation (Elev). Here we present independent variables with model support of 0.60 and higher (see Appendix S3 for all independent variables).

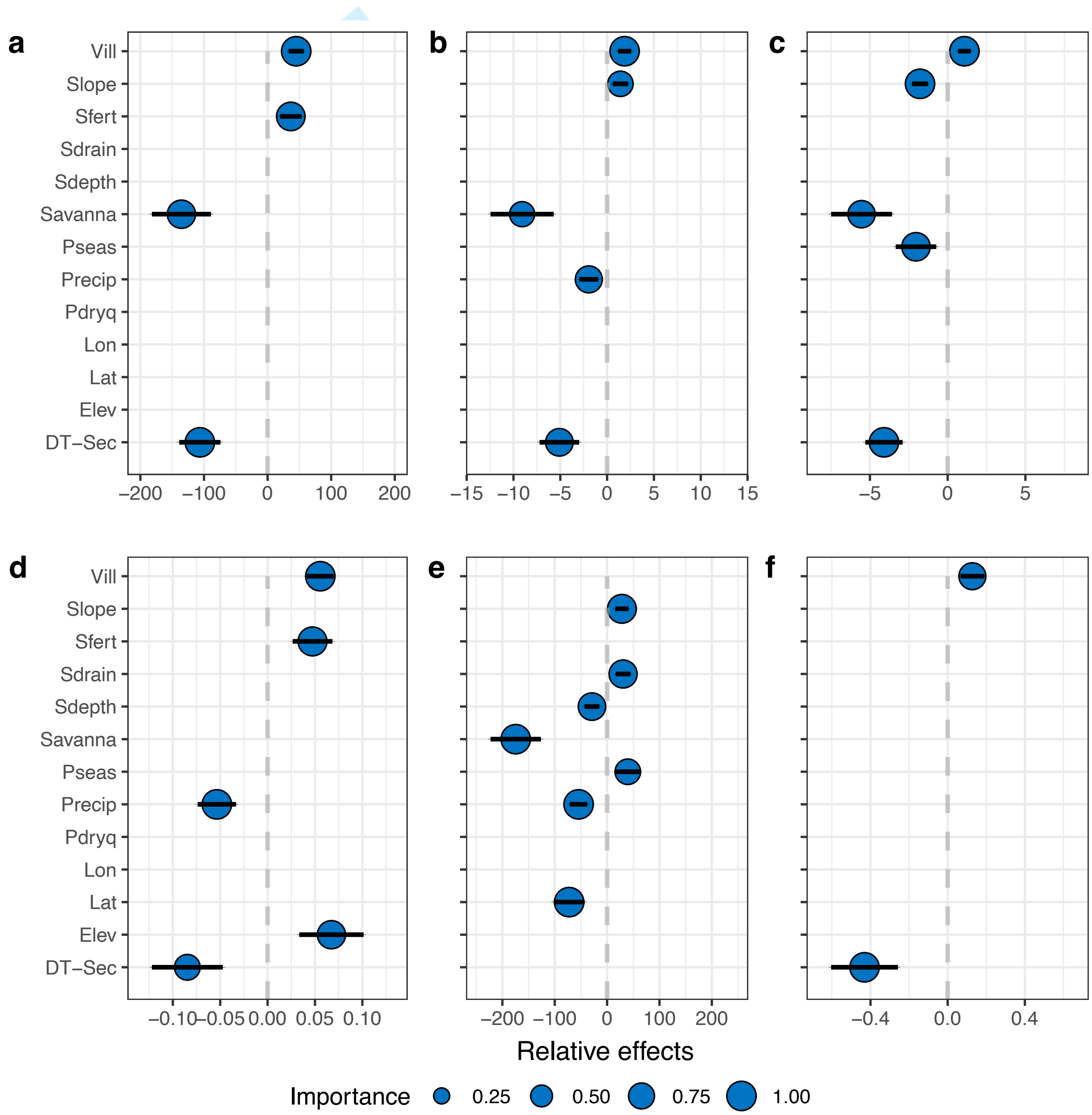

Appendix S1

Here we provide additional information on the distribution of AGC, numbers of large trees, and stand-level variables (basal area, wood density, tree height, stem density) in Gabon based on 104 NRI sites (Fig. S1.1, S1.2) and broken down by disturbance type (Fig. S1.3, S1.4). AGC per site varies by disturbance, ecosystem, habitat, and management (Fig. S1.5). We also demonstrate the relationship between AGC and the other stand variables (Fig. S1.6).

To verify our calculations of AGC, after completing our analyses (Methods, Calculation of AGC), we used the R package, BIOMASS, to re-analyze the data (Réjou-Méchain et al. 2017). BIOMASS assigns wood density values to trees, builds a local D:H allometry from five potential models, and propagates errors associated with diameter and wood density measurements, tree height predictions, and the allometric model. Results for plot-level AGC from our approach and the BIOMASS package were very similar (RMSE = 12.96).

For Peer Review

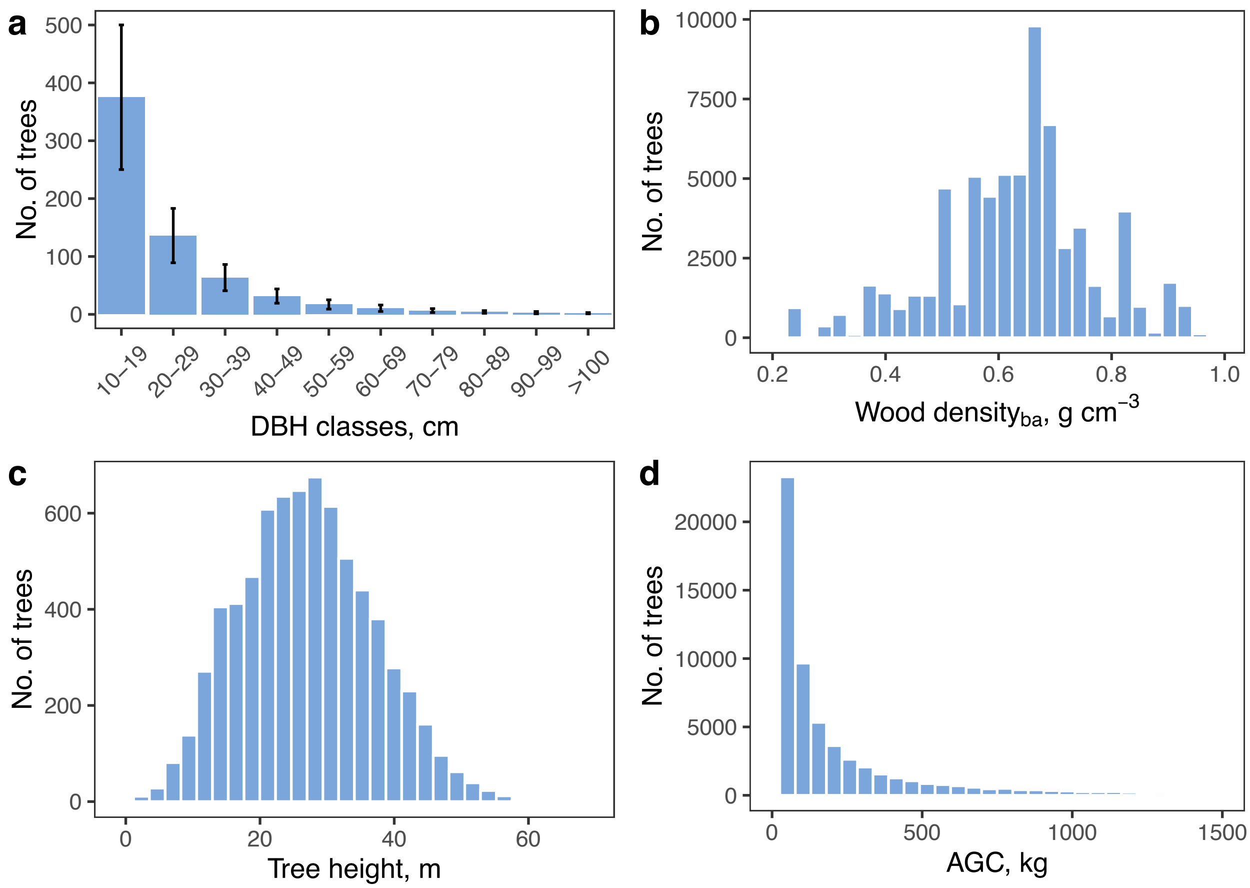

Figure S1.1. Number of trees (No. of trees) by stand characteristics, including: (a) stem density (ha^{-1}) over DBH (cm) classes (error bars are standard errors); (b) distribution of basal area-weighted wood density (g cm^{-3}) of all trees; (c) distribution of heights (m) of trees with field-based tree height measurements; and, (d) distribution of tree AGC (Mg).

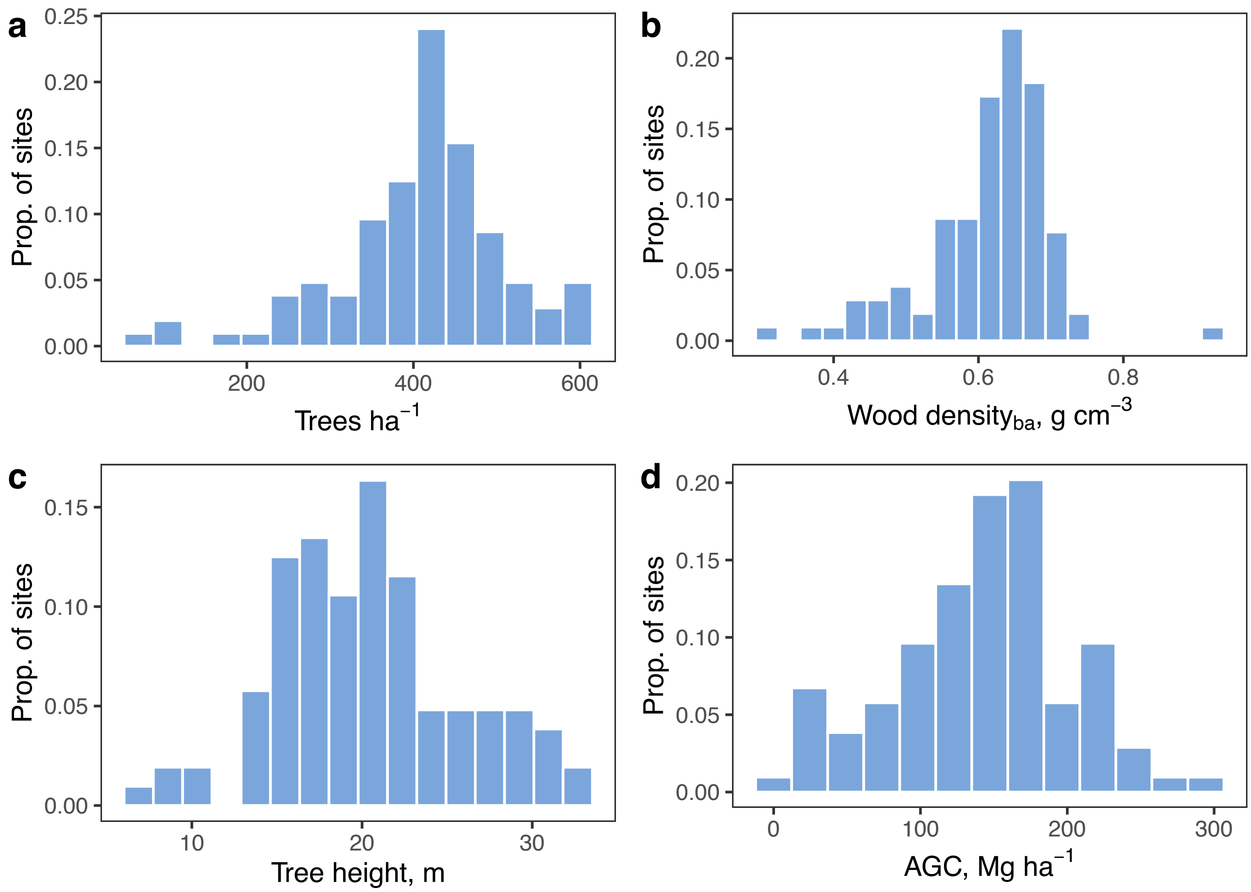

Figure S1.2. Proportion of all NRI sites (Prop. of sites) by stand characteristics, including: (a) mean stem density (stems ha^{-1}); (b) mean tree height (m ha^{-1}) of trees with field-based tree height measurements; (c) mean basal area-weighted wood density (g cm^{-3} ha^{-1}); and, (d) AGC at the site-level (Mg ha^{-1}).

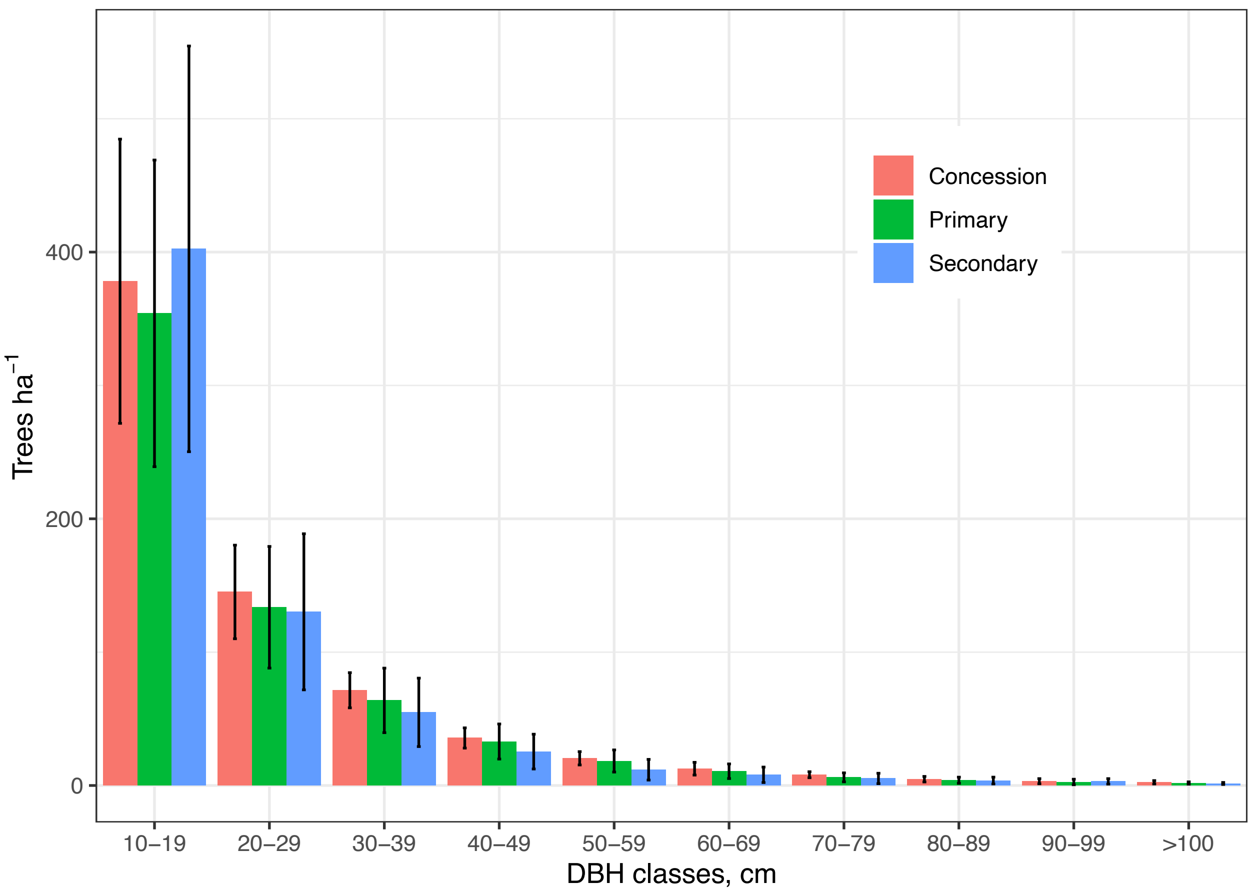

Figure S1.3. Mean stem densities (ha^{-1}) over the range of DBH (cm) classes (error bars are standard errors) for each disturbance type.

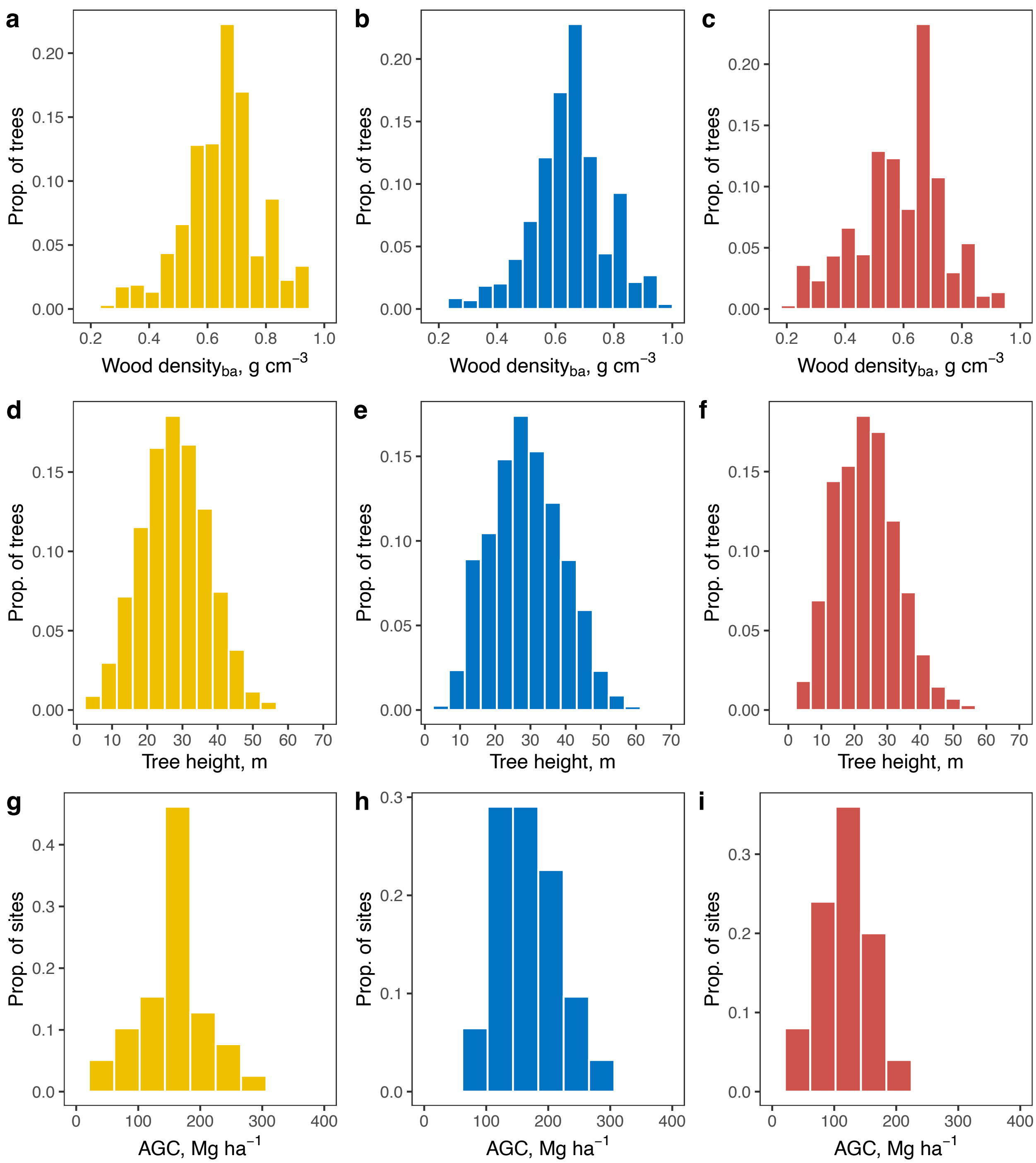

Figure S1.4. Proportion of trees (Prop. of trees) in NRI sites by stand characteristics and disturbance type, including: (a-c) distribution of heights (m) of trees with field-based tree height measurements; (d-f) distribution of wood density (g cm^{-3}) of all trees; and, (g-i) distribution of AGC at the site-level (Mg ha^{-1}). Colors represent disturbance types (yellow = primary, blue = concession, and red = secondary).

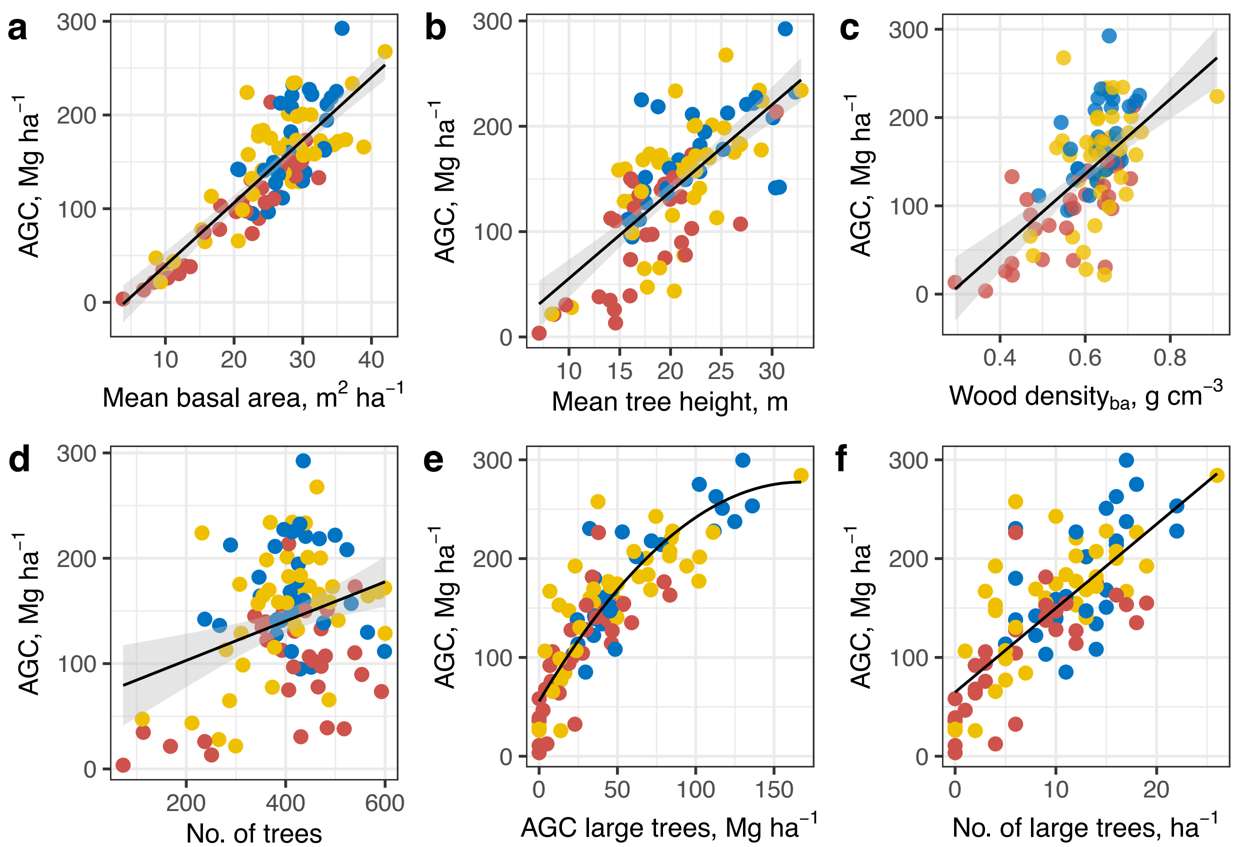

Figure S1.5. Aboveground carbon plotted against (a) basal area ($F_{1,102} = 232.8, p < 0.001, R^2 = 0.695$); (b) tree height ($F_{1,102} = 115, p < 0.001, R^2 = 0.53$); (c) basal area weighted wood mass density ($F_{1,102} = 74.04, p < 0.001, R^2 = 0.421$), (d) stem density ($F_{1,102} = 11.5, p = 0.01, R^2 = 0.101$), and (e) number of big trees ($F_{1,102} = 133, p < 0.001, R^2 = 0.561$) for the 104 NRI plots. Lines represent the best-fit regression line with their 95% confidence intervals (shading).

References

Réjou-Méchain, Maxime, Ariane Tanguy, Camille Piponiot, Jérôme Chave, and Bruno Hérault. 2017. "Biomass: an R Package for Estimating Above-Ground Biomass and Its Uncertainty in Tropical Forests." *Methods in Ecology and Evolution* 8 (9): 1163–7. https://doi.org/10.1111/2041-210X.12753.

For Peer Review

Appendix S2

Here we provide additional information related to large trees and differences among disturbance types. Most of the AGC in Gabon's forests is concentrated in a small number of large trees (Fig. S2.6).

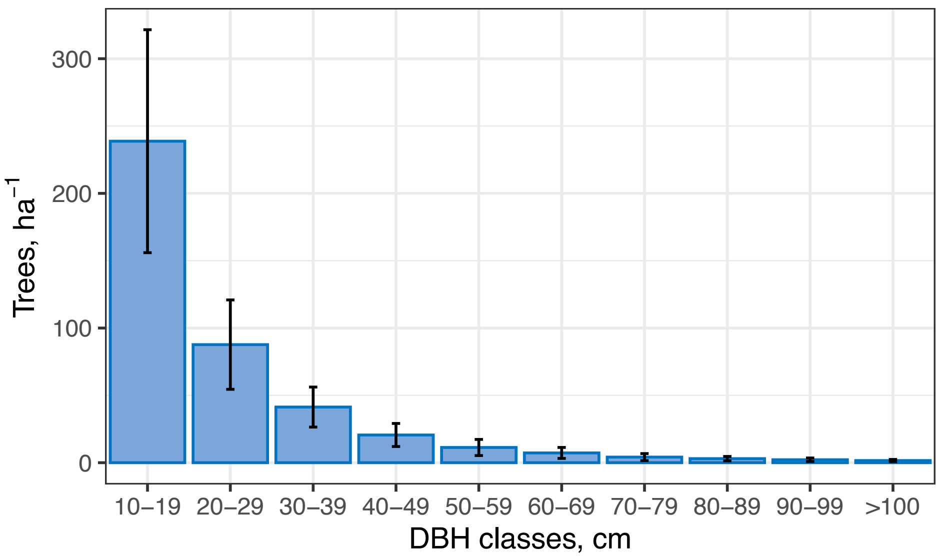

Figure S2.6. The mean number of trees per plot by diameter class. Error bars are standard deviations.

Species	Primary Forest	Concession Forest	Secondary Forest
Santiria trimera	18.90	19.10	18.30
Dichostemma glaucescens	16.60	9.60	14.90
Plagiostyles africana	12.90	14.60	15.40
Coelocaryon preussii	7.70	6.80	10.50
Diospyros sp.	7.00	13.00	9.40
Coula edulis	6.50	6.90	3.90
Aucoumea klaineana	5.80	5.70	19.20
Raphia sp.	5.70	0.00	0.00
Cola sp.	5.50	4.20	2.20
Strombosiopsis tetrandra	5.40	7.60	2.00
Heisteria parvifolia	4.50	6.20	3.10
Pentaclethra eetveldeana	4.20	6.00	6.30
Scyphocephalium ochocoa	3.90	6.90	4.50
Garcinia sp.	3.70	6.80	1.20
Staudtia gabonensis	2.80	4.00	5.10
Musanga cecropioides	1.10	3.50	16.50
Nauclea sp.	0.70	3.20	7.20

Table S2.1. Ten most abundant species for each disturbance type. Values are average number of stems ha^{-1}.

Species	Central Forest	Coastal Forest	Congolian Forest	Savannah Forest
Aucoumea klaineana	1.50	2.20	0.00	1.30
Scyphocephalium ochocoa	1.20	0.10	0.30	0.00
Desbordesia glaucescens	0.40	0.60	0.00	0.00
Dacryodes buettneri	0.30	0.20	0.20	0.20
Pycnanthus angolensis	0.30	0.10	0.30	0.50
Pterocarpus soyauxii	0.30	0.20	0.10	0.00
Sinderopsis letestui	0.30	0.10	0.00	0.00
Paraberlinia bifoliolata	0.30	0.00	0.00	0.00
Dialium pachyphyllum	0.20	0.00	0.10	0.00
Piptadeniastrum africanum	0.20	0.40	0.30	0.30
Celtis tessmannii	0.20	0.10	0.00	0.80
Scyphocephalium mannii	0.10	0.10	0.40	0.00
Pentaclethra macrophylla	0.10	0.10	0.30	0.20
Odyendyea gabonensis	0.10	0.40	0.10	0.20
Petersianthus macrocarpus	0.10	0.00	0.30	0.00
Cylicodiscus gabunensis	0.10	0.00	0.30	0.00
Erythrophleum ivorense	0.10	0.10	0.30	0.20
Mytragyna ciliata	0.00	0.20	0.20	0.20
Maranthes glabra	0.00	0.00	0.30	0.00
Gilbertiodendron dewevrei	0.00	0.00	0.50	0.00
Sacoglottis gabonensis	0.00	0.40	0.00	1.00
Rhizophora mangle	0.00	0.20	0.00	0.00
Guibourtia pelleriniana	0.00	0.20	0.00	0.00
Ceiba pentandra	0.00	0.00	0.10	0.30
Sterculia tragacantha	0.00	0.00	0.00	0.30

Table S2.2. Ten most abundant species of large trees for each ecosystem type. Values are average number of stems ha^{-1}.

Species	Primary Forest	Concession Forest	Secondary Forest
Aucoumea klaineana	1.45	1.55	1.40
Scyphocephalium ochocoa	0.52	0.84	0.72
Sacoglottis gabonensis	0.42	0.03	0.00
Sinderopsis letestui	0.35	0.06	0.00
Odyendyea gabonensis	0.30	0.19	0.04
Piptadeniastrum africanum	0.25	0.39	0.16
Scyphocephalium mannii	0.25	0.10	0.08
Gilbertiodendron dewevrei	0.22	0.00	0.00
Erythrophleum ivorense	0.20	0.10	0.04
Petersianthus macrocarpus	0.20	0.03	0.08
Pycnanthus angolensis	0.18	0.45	0.20
Pterocarpus soyauxii	0.18	0.32	0.12
Desbordesia glaucescens	0.15	0.84	0.16
Dacryodes buettneri	0.15	0.42	0.24
Celtis tessmannii	0.12	0.23	0.20
Staudtia gabonensis	0.08	0.03	0.16
Distemonanthus benthamianus	0.05	0.26	0.12
Paraberlinia bifoliolata	0.02	0.00	0.48

Table S2.3. Ten most abundant species of large trees for each disturbance type. Values are average number of large stems ha^{-1}.

For Peer Review

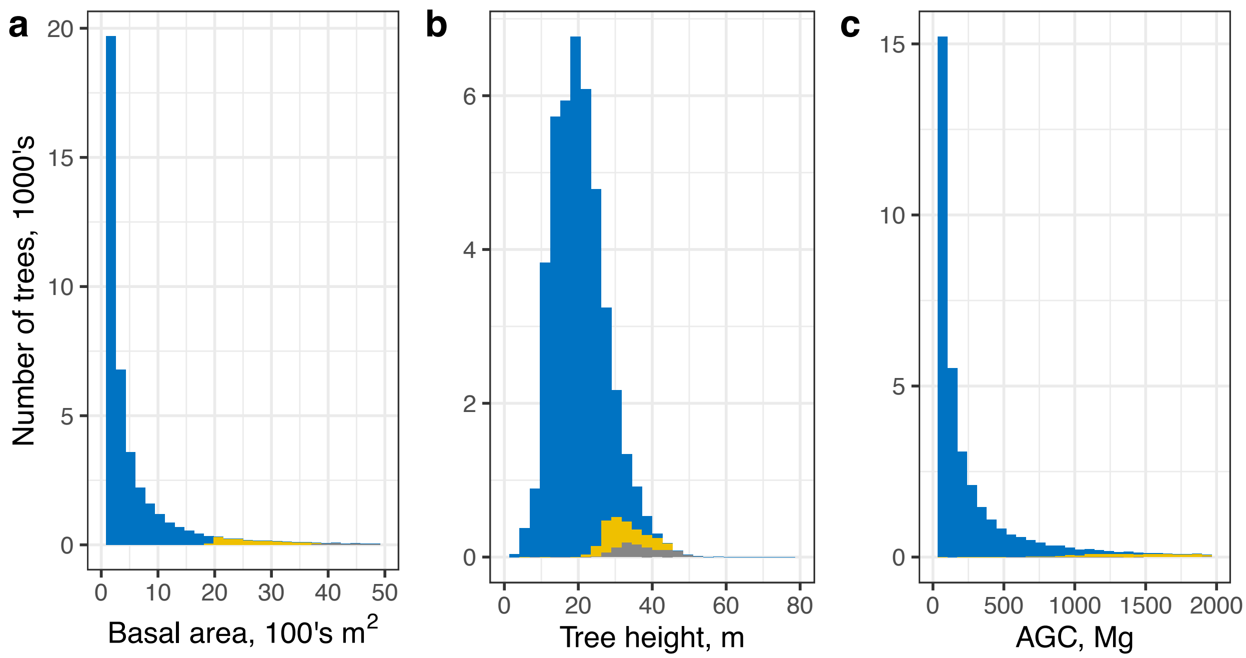

Figure S2.7. Distributions of (a) tree AGC (Mg), (b) basal area (m^2), and (c) tree heights (m) highlighting tree diameters $\geq$ 50 cm (yellow) and $\geq$ 70 cm (grey).

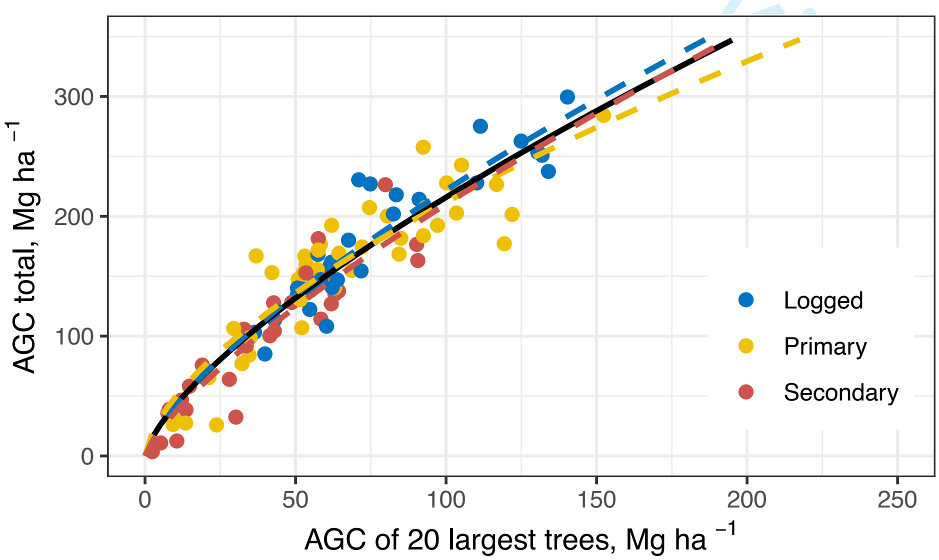

Figure S2.8. AGC of the largest trees versus the total AGC of 1-ha plots for each disturbance type and all plots combined (black dashed line).

N	α	β	R^2	RMSE	rRSE	N	α	β	R^2	RMSE	rRSE
6	453.50	0.59	0.77	68281.00	0.22	28	44.20	0.74	0.89	45769.00	0.15
7	370.40	0.61	0.78	66457.00	0.21	29	41.90	0.75	0.90	45227.00	0.14
8	311.70	0.62	0.79	64901.00	0.21	30	39.90	0.75	0.90	44704.00	0.14
9	264.90	0.63	0.80	63238.00	0.20	31	37.90	0.76	0.90	44185.00	0.14
10	229.20	0.64	0.81	61791.00	0.20	32	36.00	0.76	0.90	43670.00	0.14
11	200.00	0.65	0.82	60421.00	0.19	33	34.20	0.76	0.91	43169.00	0.14
12	174.20	0.65	0.82	58996.00	0.19	34	32.60	0.77	0.91	42680.00	0.14
13	152.80	0.66	0.83	57619.00	0.18	35	31.10	0.77	0.91	42213.00	0.14
14	135.10	0.67	0.84	56420.00	0.18	36	29.80	0.77	0.91	41753.00	0.13
15	120.60	0.68	0.85	55301.00	0.18	37	28.50	0.77	0.91	41306.00	0.13
16	108.10	0.69	0.85	54258.00	0.17	38	27.30	0.78	0.92	40877.00	0.13
17	97.80	0.69	0.86	53315.00	0.17	39	26.10	0.78	0.92	40452.00	0.13
18	89.10	0.70	0.86	52439.00	0.17	40	25.10	0.78	0.92	40034.00	0.13
19	81.40	0.70	0.87	51574.00	0.17	41	24.00	0.79	0.92	39615.00	0.13
20	74.70	0.71	0.87	50739.00	0.16	42	23.10	0.79	0.92	39205.00	0.13
21	69.00	0.72	0.87	50004.00	0.16	43	22.20	0.79	0.92	38813.00	0.12
22	64.00	0.72	0.88	49325.00	0.16	44	21.40	0.79	0.93	38427.00	0.12
23	59.60	0.73	0.88	48672.00	0.16	45	20.60	0.80	0.93	38054.00	0.12
24	55.80	0.73	0.88	48041.00	0.15	46	19.90	0.80	0.93	37683.00	0.12
25	52.50	0.73	0.89	47461.00	0.15	47	19.20	0.80	0.93	37319.00	0.12
26	49.40	0.74	0.89	46893.00	0.15	48	18.50	0.80	0.93	36965.00	0.12
27	46.60	0.74	0.89	46318.00	0.15	49	17.90	0.81	0.93	36624.00	0.12

Table S2.4. Coefficent values for the Bastin model using the entire dataset, including N, the number of largest trees, α, β, R^2, RMSE (root mean square error), and rRSE (relative root square error).

For Peer Review

Model	a	b	c	AICc	AICc Gabon
Logged	1.03	10.44	25.99	-3572.57	-2444.27
Primary	1.02	7.21	7.50	-3968.68	-2128.15
Secondary	1.01	2.78	6.50	-4117.54	-2363.09

Table S2.5. Comparison of model parameters and AICc scores among different disturbance types and the general *Gabon model*, with parameters $a = 1.01$, $b = 4.78$ and $c = 9.03$.

Appendix S3

Here we provide additional information on the climatic, edaphic and anthropogenic variables that drive spatial patterns of AGC and large trees in Gabon based on 104 1-ha NRI plots. Results of the principal components analyses demonstrate our reductions of multiple climatic and edaphic variables to three linearly uncorrelated variables (Tables S3.6 and S3.7). We also show the bivariate relationships among independent variables and six response variables (AGC, basal area, wood density, tree height, stem density, and number of big trees; Figures S3.11 - S3.16). Below we describe the effects of environmental and anthropogenic variables on stand variables and provide the results of model averaging for AGC, numbers of large trees, and all stand variables (basal area, tree height, wood density, stem density), showing the effects of independent variables as coefficients and standardized coefficients (Table S3.8): these results make up Fig. 6 in the main text.

In Gabon's forests, variation in basal area was most strongly influenced by savanna ecosystems and secondary forests, both of which are characterized by having few large trees relative to other ecosystem and less disturbed forest types. Basal area also decreased with annual precipitation. This result differs from previous reports that basal area decreases proportionally to increases in dry season length due to water stress (Malhi et al. 2006; Baraloto et al. 2011). However, like Lewis et al. (2013), ever-wet forests tend to have lower AGC, implying that excess rainfall either reduces net primary productivity or elevates mortality. Finally, basal area also increased slightly on slopes, which might reflect a lower abundance of large trees in low-lying swamps and streams or that large basal area provides better structural support on slopes.

Wood density increased with elevation, which controls soil chemistry and hydrology and can profoundly influence forest structure (Jucker et al. 2018). Trees on ridges and at higher elevations could have higher wood density as competition for nutrients and water favors species with life-history traits that maximize survival rather than rapid growth (Werner and Homeier 2015). However, similar to Lewis et al. (Lewis et al. 2013), we also found that wood density increased with soil fertility contrary to predictions that competitive, fast-growing species would dominate resource rich sites (Malhi et al. 2006; Gourlet-Fleury et al. 2011). Annual precipitation negatively affected wood density, providing evidence to findings that wood density is correlated with drought tolerance (Slik 2004). West African rainforest trees also demonstrated a positive relationship between wood density and precipitation with high wood density possibly providing greater structural stability and greater resistance against physical damage and pathogens in the shaded understory (Maharjan et al. 2011).

Tree height tended to be negatively affected by slope and especially by seasonality of precipitation. The decline of tree height with slope is consistent with empirical evidence highlighting strong shifts in carbon allocation strategies and crown architecture of trees as soil nutrients and water availability become limiting (Jucker et al. 2018). Soil mineral layers on slopes are likely to be thinner, more waterlogged and generally less favorable for root development (Quesada et al. 2012), providing little mechanical support for tall trees. Tall trees are at higher risk of falling or being blown over on slopes as wind speeds increase with altitude on mountains and proximity to ridges (Woodward 1993). Lawton (1982) found that for a given tree height, trunk diameter increases with proximity to the ridge-crest (which might also explain increasing basal area with slope above). In terms of seasonality in precipitation, Feldpausch et al. (2012) found dry-season length was a key factor influencing height-diameter relationships, with a longer dry season being associated with stouter trees. Greater stem diameter relative to tree height may serve to increase overall rates of water transport due to higher sapwood cross-sectional areas (Meinzer, Goldstein, and Andrade 2001).

Stem density was only weakly affected by environmental variables, increasing with slope, seasonality of precipitation, and soil drainage and decreasing with annual precipitation and soil depth. Stem density likely increases with slope because large trees are limited by soil, water, and mechanical support, opening space for higher numbers of smaller trees. The effects of climate and soil are difficult to explain. In contrast to our results, previous studies in the Amazon and Borneo have found stem density to be negatively correlated with seasonality and positively correlated with annual rainfall (Steege et al. 2013; Slik et al. 2010). In Borneo, stem density decreased with soil depth like this study, but decreased with better drainage (Slik et al. 2010). Environmental variables may have a weak effect on stem density; Lewis et al. (Lewis et al. 2013) suggested that stem density in African old-growth forests is largely an emergent property of a disturbance regime favoring low stem turnover, long carbon residence times and high ACG.

Table S3.6. Principal components analysis (PCA) factor loadings for the three climate axes.

Factor	Axis 1	Axis 2	Axis 3
Mean temp, °C	-0.415	-0.2646	-0.2982
Mean temp, warmest quarter, °C	-0.4379	-0.1506	-0.2885
Mean temp, coldest quarter, °C	-0.3098	-0.5003	-0.299
Seasonality, temp, °C	-0.331	0.4999	-0.0428
Annual precip, mm	-0.2572	-0.2602	0.6147
Wettest quarter, mm	-0.2992	-0.1892	0.5941
Driest quarter, mm	0.3571	-0.3788	0.0205
Seasonality, precip, mm	-0.3838	0.4001	0.0738

For Peer Review

Table S3.7. Principal components analysis (PCA) factor loadings for the three soil axes.

Factor	Axis 1	Axis 2	Axis 3
Base saturation topsoil	0.286	0.29137	-0.28897
CEC clay topsoil	0.33891	0.14668	-0.23572
CEC soil topsoil	0.36488	-0.11283	-0.01124
Organic carbon topsoil	0.37075	-0.16115	-0.02905
Organic carbon subsoil	0.37343	-0.11922	-0.08309
pH topsoil	0.23151	0.42438	-0.00676
Textural class topsoil	0.22994	0.01152	0.4899
Textural class subsoil	0.12939	0.07326	0.3153
Soil drainage	0.11046	-0.18725	0.54331
Effective soil depth	0.00316	0.50481	0.05653
Easy available water	-0.08545	0.49298	0.18522
Nitrogen topsoil	0.32568	-0.20491	0.16721
C:N ratio topsoil	0.0887	-0.24602	-0.39054
Soil production index	0.36966	0.14011	-0.02062

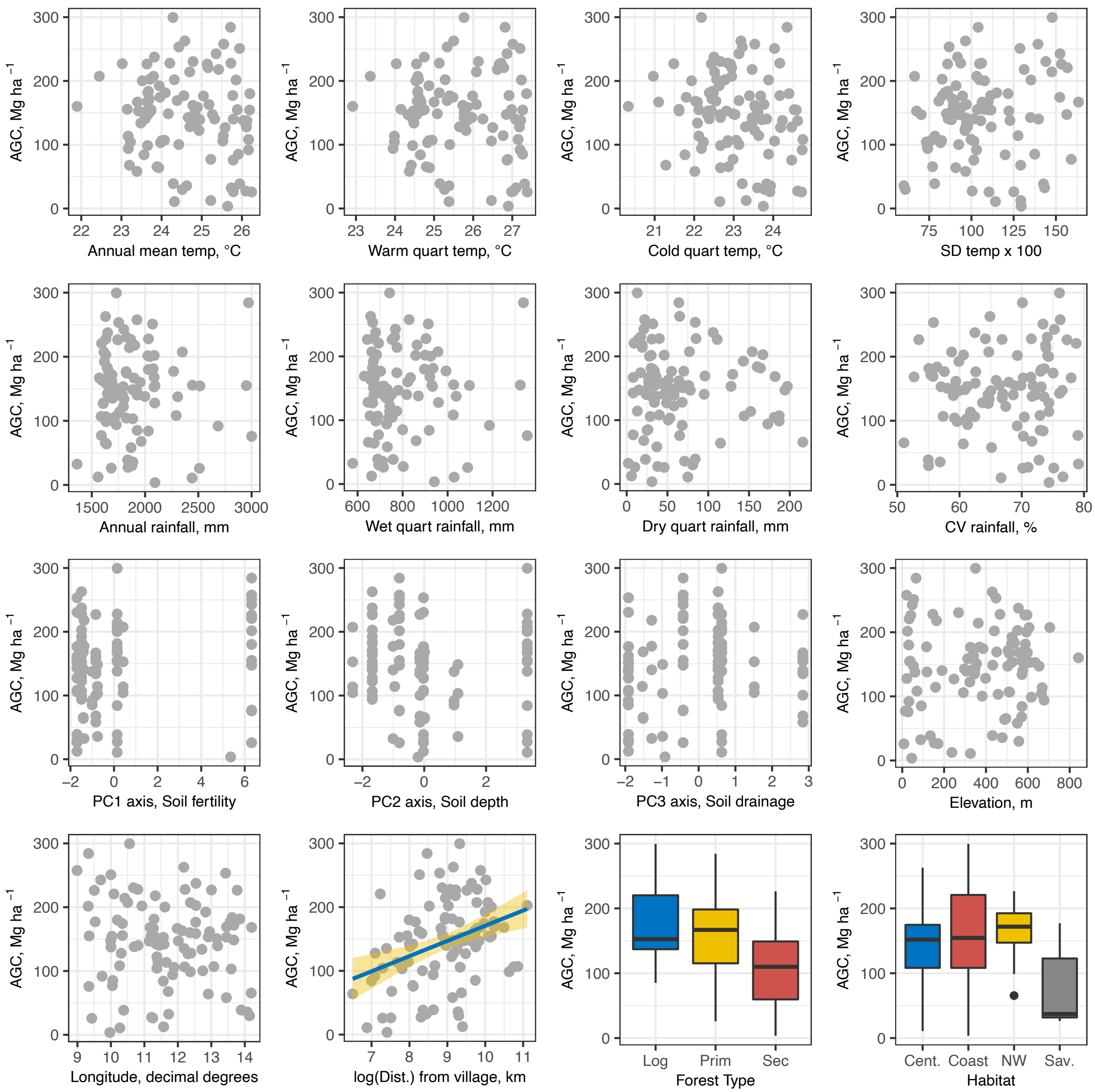

Figure S3.9. Bivariate plots of AGC versus (a) temperature, top (annual mean temperature, temperature in warmest quarter, temperature in coldest quarter, standard deviation (SD) of temperature); (b) rainfall, second row (annual rainfall, rainfall in wettest quarter, rainfall in driest quarter, coefficient of variation (CV) of rainfall); (c) soil and elevation, third row (PC axis 1, PC axis 2, PC axis 3, elevation); (d) geography and disturbance, bottom (latitude, longitude, distance from village, and forest type). Fit lines represent a significant relationship, and shading is the 95% CI around the line.

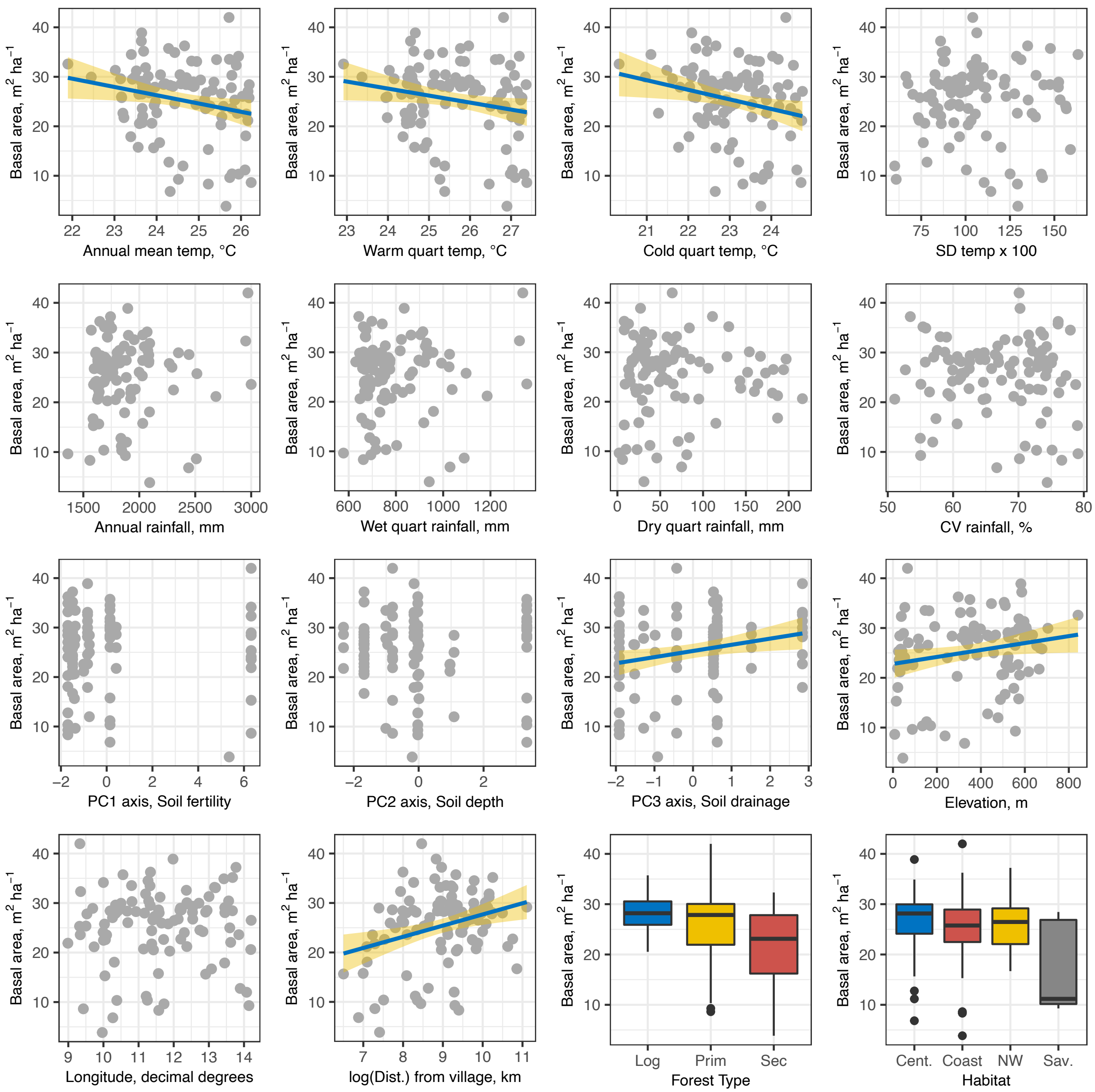

Figure S3.10. Bivariate plots of basal area versus (a) temperature, top (annual mean temperature, temperature in warmest quarter, temperature in coldest quarter, standard deviation (SD) of temperature); (b) rainfall, second row (annual rainfall, rainfall in wettest quarter, rainfall in driest quarter, coefficient of variation (CV) of rainfall); (c) soil and elevation, third row (PC axis 1, PC axis 2, PC axis 3, elevation); (d) geography and disturbance, bottom (latitude, longitude, distance from village, and forest type). Fit lines represent a significant relationship, and shading is the 95% CI around the line.

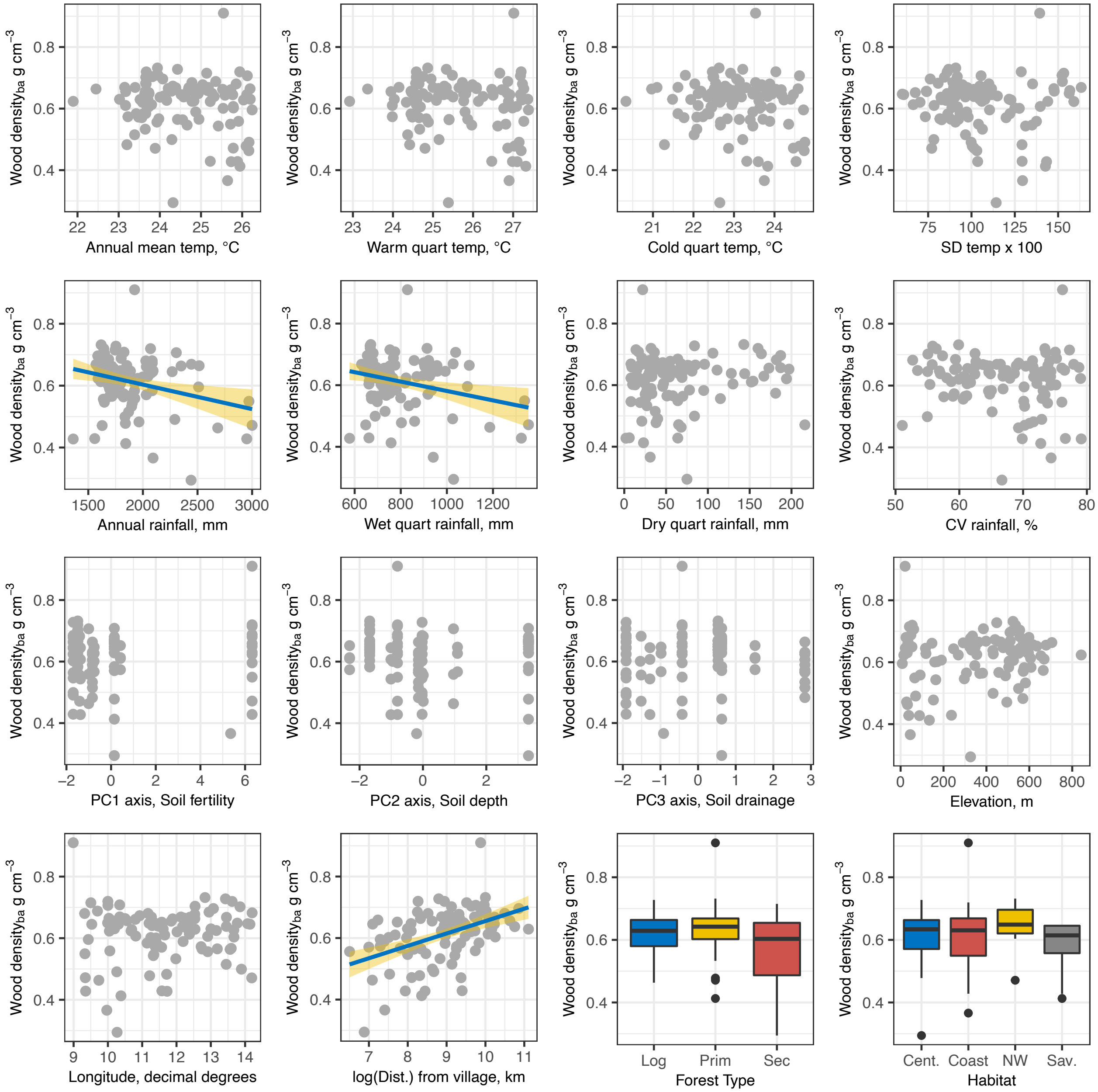

Figure S3.11. Bivariate plots of basal area-weighted wood density versus (a) temperature, top (annual mean temperature, temperature in warmest quarter, temperature in coldest quarter, standard deviation (SD) of temperature); (b) rainfall, second row (annual rainfall, rainfall in wettest quarter, rainfall in driest quarter, coefficient of variation (CV) of rainfall); (c) soil and elevation, third row (PC axis 1, PC axis 2, PC axis 3, elevation); (d) geography and disturbance, bottom (latitude, longitude, distance from village, and forest type). Fit lines represent a significant relationship, and shading is the 95% CI around the line.

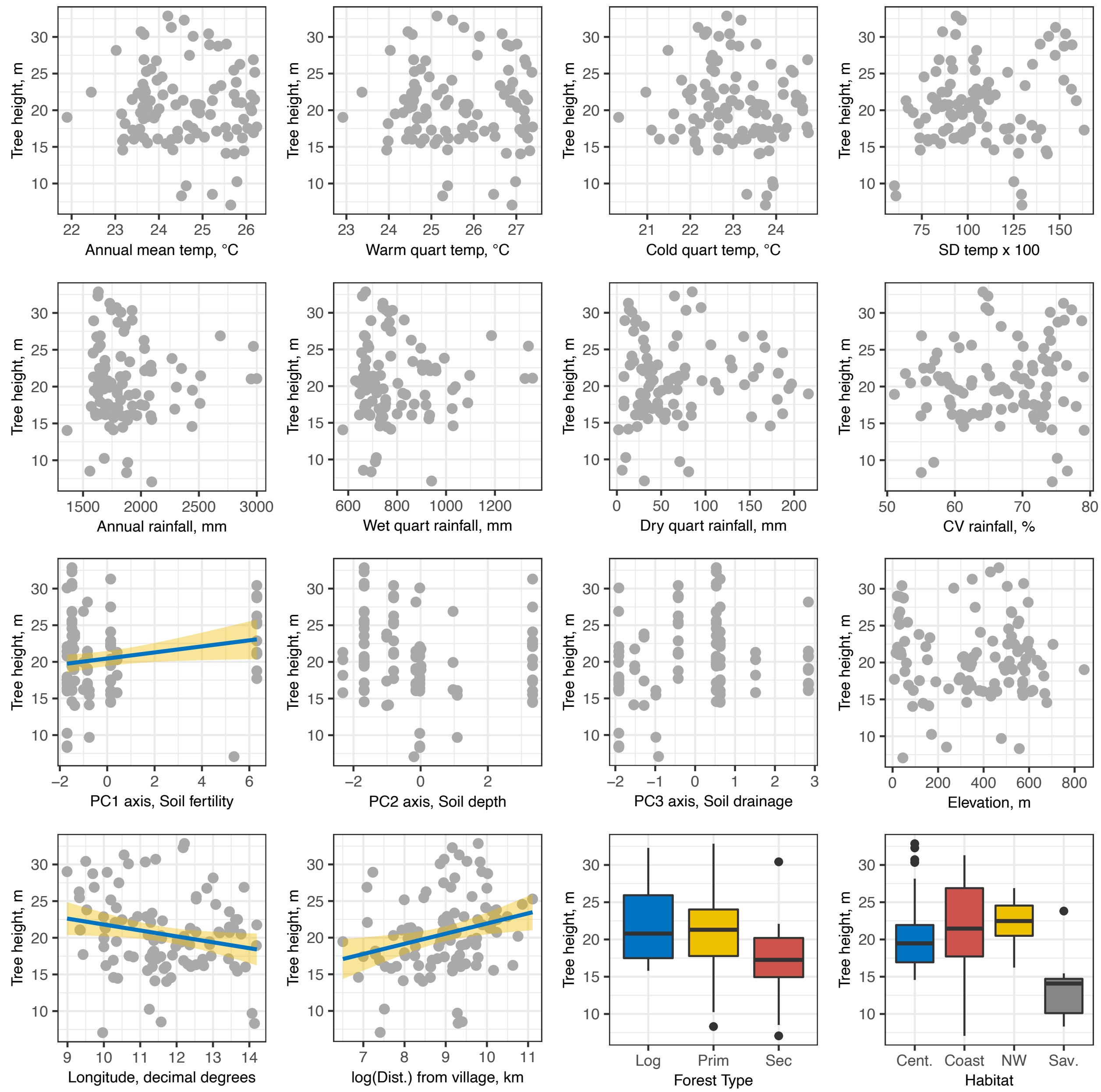

Figure S3.12. Bivariate plots of tree height versus (a) temperature, top (annual mean temperature, temperature in warmest quarter, temperature in coldest quarter, standard deviation (SD) of temperature); (b) rainfall, second row (annual rainfall, rainfall in wettest quarter, rainfall in driest quarter, coefficient of variation (CV) of rainfall); (c) soil and elevation, third row (PC axis 1, PC axis 2, PC axis 3, elevation); (d) geography and disturbance, bottom (latitude, longitude, distance from village, and forest type). Fit lines represent a significant relationship, and shading is the 95% CI around the line.

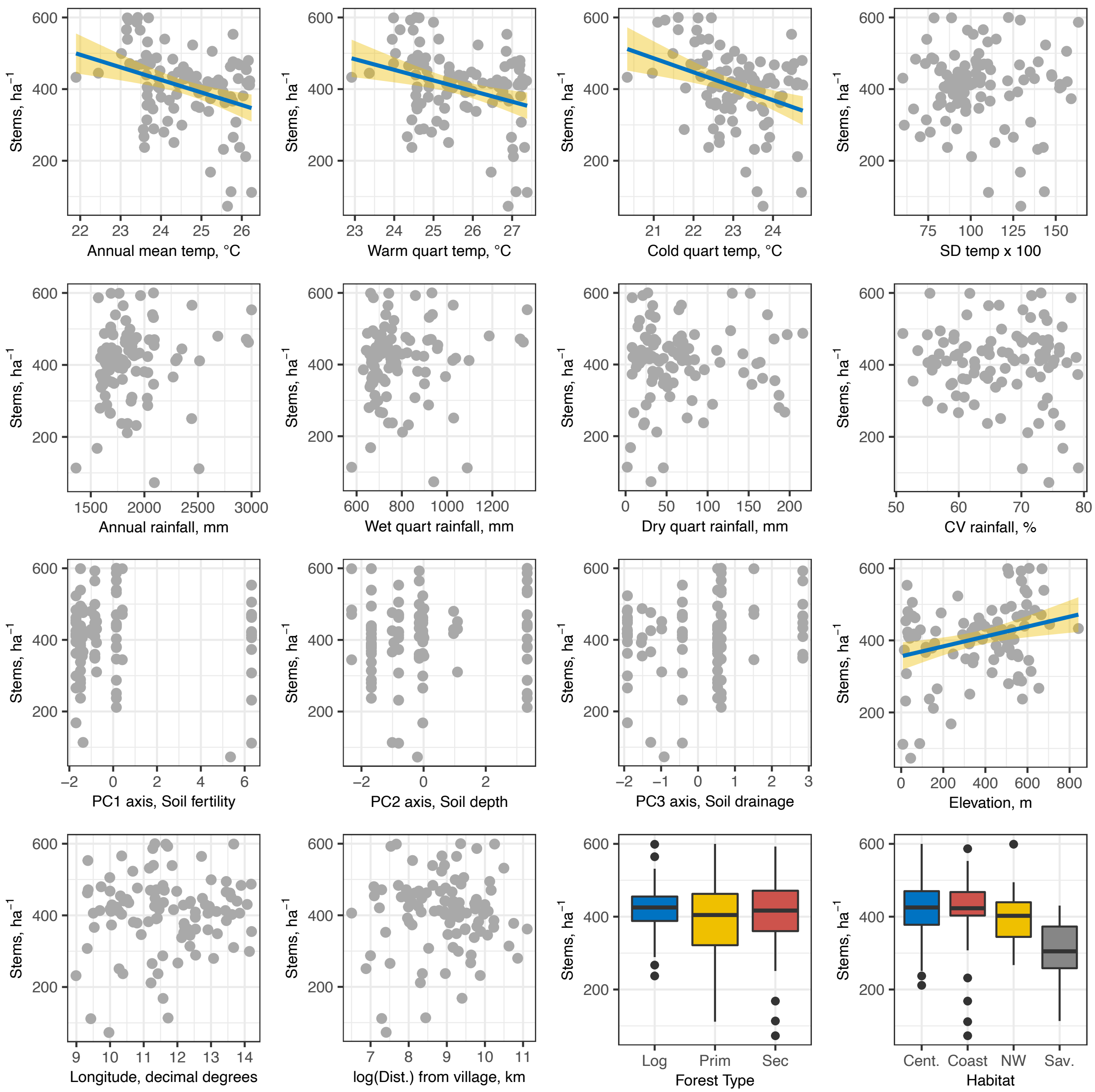

Figure S3.13. Bivariate plots of stem density versus (a) temperature, top (annual mean temperature, temperature in warmest quarter, temperature in coldest quarter, standard deviation (SD) of temperature); (b) rainfall, second row (annual rainfall, rainfall in wettest quarter, rainfall in driest quarter, coefficient of variation (CV) of rainfall); (c) soil and elevation, third row (PC axis 1, PC axis 2, PC axis 3, elevation); (d) geography and disturbance, bottom (latitude, longitude, distance from village, and forest type). Fit lines represent a significant relationship, and shading is the 95% CI around the line.

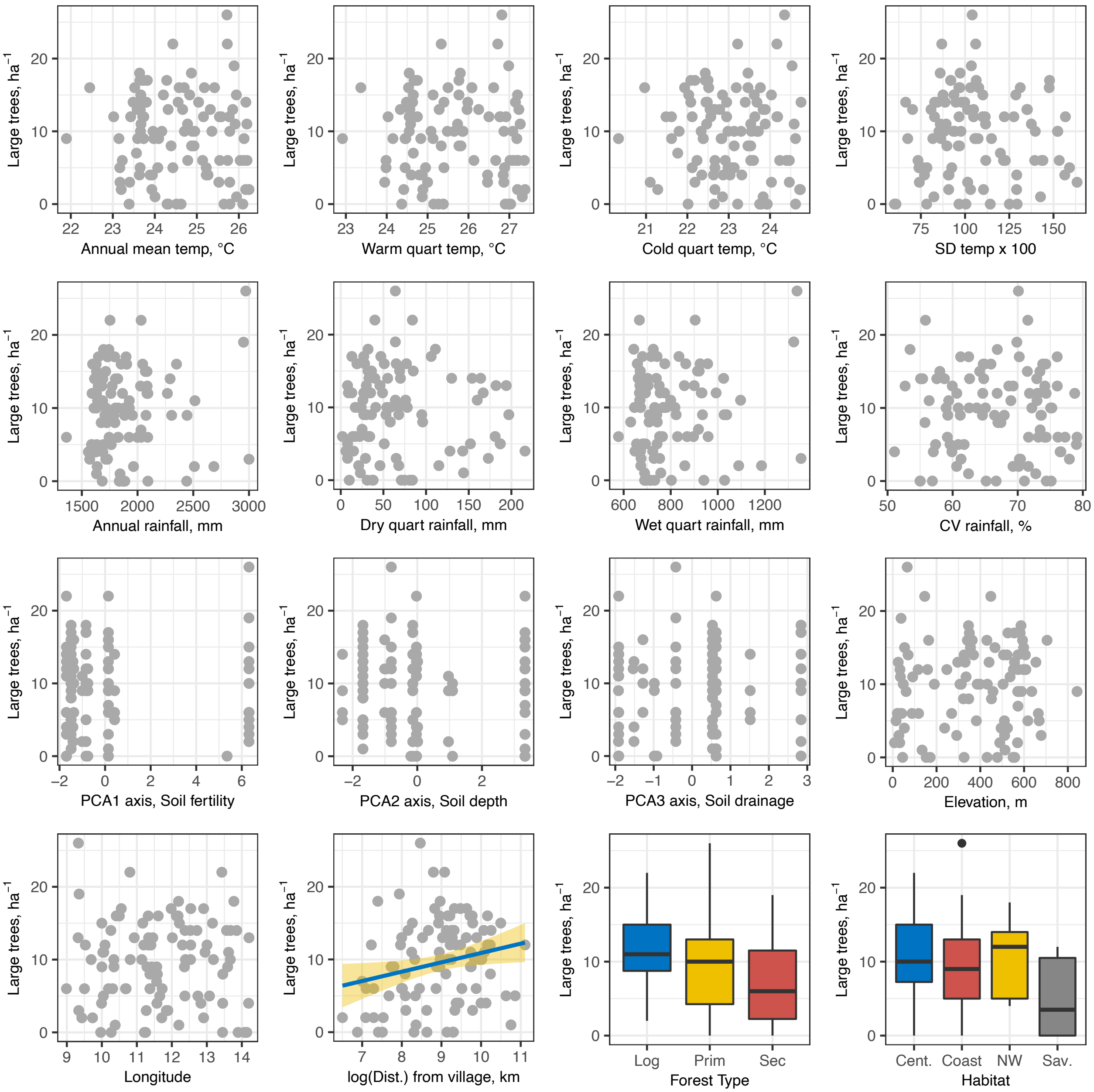

Figure S3.14. Bivariate plots of number of large trees ($\geq$ 70 cm dbh) versus (a) temperature, top (annual mean temperature, temperature in warmest quarter, temperature in coldest quarter, standard deviation (SD) of temperature); (b) rainfall, second row (annual rainfall, rainfall in wettest quarter, rainfall in driest quarter, coefficient of variation (CV) of rainfall); (c) soil and elevation, third row (PC axis 1, PC axis 2, PC axis 3, elevation); (d) geography and disturbance, bottom (latitude, longitude, distance from village, and forest type). Fit lines represent a significant relationship, and shading is the 95% CI around the line.

Table S3.8. Results of model averaging for each of six response variables: aboveground carbon, mean basal area, mean tree height, mean wood density, stem density, and number of big trees. For each response variable, we provide the following: *Var.* is a list of abbreviations of independent variables in order of relative importance; *Coef.* is the regression or GLM (big trees) coefficient for the variable; *S-Coef.* is the standardized coefficient for the variable; and, *Supp.* is the relative support for each independent variable, quantified as the proportion of models in which the variable occurred.

	Aboveground carbon, Mg ha^{-1}				Basal area, m^2 ha^{-1}				Tree height, m			
	Var.	Coef.	S-Coef.	Supp.	Var.	Coef.	S-Coef.	Supp.	Var.	Coef.	S-Coef.	Supp.
1	DT-Sec	-110.01	-106.46	1.00	Vill	2.06	1.87	0.98	DT-Sec	-4.13	-4.10	1.00
2	Vill	50.40	45.00	1.00	DT-Sec	-5.34	-5.10	0.84	Vill	1.35	1.08	1.00
3	Sfert	14.35	36.53	0.93	Precip	-1.57	-1.95	0.79	Slope	-0.32	-1.78	1.00
4	Savanna	-134.19	-135.46	0.91	Slope	0.26	1.42	0.68	Pseas	-1.40	-2.04	0.92
5	Pseas	16.92	22.31	0.50	Savanna	-9.09	-9.08	0.65	Savanna	-5.58	-5.54	0.83
6	Lat	-8.14	-12.34	0.27	Sdepth	-0.98	-1.64	0.57	Elev	-0.01	-2.71	0.49
7	Sdepth	-6.95	-11.34	0.18	Lat	-1.85	-2.43	0.46	Sdrain	-0.57	-0.78	0.47
8	Sdrain	-3.72	-5.90	0.09	Pseas	0.92	1.13	0.21	Lat	1.35	2.00	0.46
9	Slope	-0.94	-5.40	0.09	Sfert	0.29	0.75	0.13	Precip	-0.87	-1.16	0.35
10	Elev	0.03	2.21	0.09	Pdryq	0.91	1.50	0.12	Lon	-0.24	-0.17	0.33
11	Precip	3.06	4.33	0.08	Elev	0.01	1.10	0.12	Pdryq	-0.59	-1.40	0.25
12	Pdryq	-1.64	-3.11	0.08	Lon	0.20	0.23	0.09	Sdepth	-0.33	-0.52	0.25
13	Lon	-4.50	-7.36	0.07	Sdrain	0.03	0.14	0.09	Sfert	0.23	0.56	0.18

	Wood $density_{ba}$, g cm^{-3}				Stem density, ha^{-1}				Big trees, ha^{-1}			
	Var.	Coef.	S-Coef.	Supp.	Var.	Coef.	S-Coef.	Supp.	Var.	Coef.	S-Coef.	Supp.
1	Precip	-0.04	-0.05	1.00	Precip	-43.28	-54.42	1.00	DT-Sec	-0.45	-0.43	0.88
2	Vill	0.06	0.06	1.00	Savanna	-174.47	-174.49	1.00	Vill	0.13	0.13	0.71
3	Sfert	0.02	0.05	0.96	Lat	-53.79	-72.43	1.00	Precip	-0.06	-0.08	0.29
4	Elev	0.00	0.07	0.90	Slope	5.04	28.27	0.95	Savanna	-0.65	-0.66	0.15
5	DT-Sec	-0.09	-0.08	0.71	Sdrain	21.27	30.56	0.89	Sdrain	-0.03	-0.04	0.13
6	Lon	-0.03	-0.04	0.41	Sdepth	-16.66	-28.90	0.84	Pdryq	0.04	0.08	0.11
7	Sdrain	-0.02	-0.02	0.34	Pseas	29.54	39.51	0.69	Elev	0.00	0.01	0.11
8	Pdryq	0.00	0.01	0.22	Elev	0.18	38.50	0.40	Pseas	0.02	0.03	0.08
9	Lat	0.01	0.01	0.13	Lon	9.99	13.87	0.24	Sfert	0.01	0.04	0.08
10	Sdepth	-0.00	-0.01	0.11	Pdryq	-7.34	-15.11	0.19	Lon	-0.01	-0.02	0.07
11	Pseas	-0.01	-0.01	0.11	Sfert	-4.66	-12.19	0.14	Sdepth	-0.01	-0.01	0.07
12	Slope	0.00	0.00	0.08	Vill	2.58	2.65	0.09	Lat	0.01	0.02	0.07
13	Savanna	-0.11	-0.11	0.04	DT-Sec	9.37	9.37	0.01	Slope	0.00	0.01	0.06

For Peer Review

References

Baraloto, Christopher, Suzanne Rabaud, Quentin Molto, Lilian Blanc, Claire Fortunel, Bruno Hérault, Nallarett Dávila, et al. 2011. "Disentangling stand and environmental correlates of aboveground biomass in Amazonian forests." *Global Change Biology* 17 (8): 2677–88. https://doi.org/10.1111/j.1365-2486.2011.02432.x.

Gourlet-Fleury, Sylvie, Vivien Rossi, Maxime Rejou-Mechain, Vincent Freycon, Adeline Fayolle, Laurent Saint-André, Guillaume Cornu, et al. 2011. "Environmental filtering of dense-wooded species controls above-ground biomass stored in African moist forests." *Journal of Ecology* 99 (4): 981–90. https://doi.org/10.1111/j.1365-2745.2011.01829.x.

Jucker, Tommaso, Boris Bongalov, David F.R.P. Burslem, Reuben Nilus, Michele Dalponte, Simon L. Lewis, Oliver L. Phillips, Lan Qie, and David A. Coomes. 2018. "Topography shapes the structure, composition and function of tropical forest landscapes." *Ecology Letters*, DOI: 10.1111/ele.12964. https://doi.org/10.1111/ele.12964.

Lewis, Simon L., Bonaventure Sonké, Terry Sunderland, Serge K. Begne, Gabriela Lopez-Gonzalez, Geertje M. F. van der Heijden, Oliver L. Phillips, et al. 2013. "Above-ground biomass and structure of 260 African tropical forests." *Philosophical Transactions of the Royal Society B* 368 (1625): 1–14.

Maharjan, S.K.a B, L.a B Poorter, M.b Holmgren, F.a Bongers, J.J.c Wieringa, and W.D.d Hawthorne. 2011. "Plant functional traits and the distribution of West African rain forest trees along the rainfall gradient." *Biotropica* 43 (5): 552–61. https://doi.org/10.1111/j.1744-7429.2010.00747.x.

Malhi, Yadvinder, Daniel Wood, Timothy R. Baker, James Wright, Oliver L. Phillips, Thomas Cochrane, Patrick Meir, et al. 2006. "The regional variation of aboveground live biomass in old-growth Amazonian forests." *Global Change Biology* 12 (7): 1107–38. https://doi.org/10.1111/j.1365-2486.2006.01120.x.

Meinzer, F.C., G. Goldstein, and J.L. Andrade. 2001. "Regulation of water flux through tropical forest canopy trees Do universal rules apply?" *Tree Physiology* 21: 19–26.

Quesada, C. A., O. L. Phillips, M. Schwarz, C. I. Czimczik, T. R. Baker, S. Patiño, N. M. Fyllas, et al. 2012. "Basin-wide variations in Amazon forest structure and function are mediated by both soils and climate." *Biogeosciences* 9 (6): 2203–46. https://doi.org/10.5194/bg-9-2203-2012.

Slik, J. W.F. 2004. "El Niño droughts and their effects on tree species composition and diversity in tropical rain forests." *Oecologia* 141 (1): 114–20. https://doi.org/10.1007/s00442-004-1635-y.

Slik, J. W.F., Shin Ichiro Aiba, Francis Q. Brearley, Chuck H. Cannon, Olle Forshed, Kanehiro Kitayama, Hidetoshi Nagamasu, et al. 2010. "Environmental correlates of tree biomass, basal area, wood specific gravity and stem density gradients in Borneo's tropical forests." *Global Ecology and Biogeography* 19 (1): 50–60. https://doi.org/10.1111/j.1466-8238.2009.00489.x.

Steege, Hans ter, Nigel C.A. Pitman, Daniel Sabatier, Christopher Baraloto, Rafael P. Salomão, Juan Ernesto Guevara, Oliver L. Phillips, et al. 2013. "Hyperdominance in the Amazonian tree flora." *Science* 342: 1243092. https://doi.org/10.1126/science.1243092.

Werner, Florian A., and Jürgen Homeier. 2015. "Is tropical montane forest heterogeneity promoted by a resource-driven feedback cycle? Evidence from nutrient relations, herbivory and litter decomposition along a topographical gradient." *Functional Ecology* 29 (3): 430–40. https://doi.org/10.1111/1365-2435.12351.

Woodward, F. I. 1993. "The Lowland-to-Upland Transition - Modelling Plant Responses to Environmental Change." *Ecological Applications* 3 (3): 404–8.

For Peer Review